M.tech (Computational Design) [Shalabh Singhal] 2018

FAULT DIAGNOSIS AND COMPUTATIONAL MODELING OF RAILWAY TRACTION SYSTEM

A DISSERTATION

SUBMITTED IN PARTIAL FULFILLMENT OF THE REQUIREMENTS

FOR THE AWARD OF THE DEGREE

OF

MASTER OF TECHNOLOGY

IN

COMPUTATIONAL DESIGN

Submitted by:

SHALABH SINGHAL

(2k16/CDN/05)

Under the supervision of

Prof. VIKAS RASTOGI

DEPARTMENT OF MECHANICAL ENGINEERING

DELHI TECHNOLOGICAL UNIVERSITY

(Formerly Delhi College of Engineering)

Bawana Road, Delhi-110042

JULY, 2018

DELHI TECHNOLOGICAL UNIVERSITY

(Formerly Delhi College of Engineering)

Bawana Road, Delhi-110042

CANDIDATE'S DECLARATION

I, Shalabh Singhal, Roll No. 2k16/CDN/05, student of M.Tech (Computational Design), hereby declare that the project Dissertation titled "Fault Diagnosis and Computational Modeling of Railway traction system" which is submitted by me to the Department of Mechanical Engineering, Delhi Technological University, Delhi in partial fulfilment of the requirement for the award of the degree of Master of Technology, is original and not copied from any source without any proper citation. This work has not previously formed the basis for the award of any Degree, Diploma Associateship, Fellowship or other similar title or recognition.

Place: Delhi **(SHALABH SINGHAL)**

Date:

DEPARTMENT OF MECHANICAL ENGINEERING

DELHI TECHNOLOGICAL UNIVERSITY

(Formerly Delhi College of Engineering)

Bawana Road, Delhi-110042

CERTIFICATE

I hereby certify that the Project Dissertation titled "Fault Diagnosis and Computational Modeling of Railway traction system " which is submitted by Shalabh Singhal, Roll No 2k16/CDN/05 Department of Mechanical Engineering, Delhi Technological University, Delhi in partial fulfilment of the requirement for the award of the degree of Master of Technology, is a record of the project work carried out by the students under my supervision. To the best of my knowledge this work has not been submitted in part or full for any Degree or Diploma to this University or elsewhere.

Place: Delhi **(Prof. VIKAS RASTOGI)**

Date: **SUPERVISOR**

ACKNOWLEDGEMENT

The satisfaction and euphoria on the successful completion of any task would be incomplete without the mention of the people who made it possible whose constant guidance and encouragement crowned out effort with success. I am grateful to the **Dept. of Mechanical Engineering, DTU**, for giving me the opportunity to execute this project, which is an integral part of the curriculum in M.Tech Programme at the Delhi Technological University, DTU.

I would like to express my deep sense of gratitude and respect to my **supervisor Prof. Vikas Rastogi** for his excellent guidance, suggestions and constant support. I consider myself extremely lucky to be able to work under the guidance of such a dynamic personality. I am also thankful to **Prof. Vipin, H.O.D, Department of Mechanical Engineering, DTU** for giving me this opportunity to carryout and complete my project.

Also I would like to thank **Mr. Anuj Sharma (research scholar)** and **Mr. Ashish Gupta (research scholar)** for all their support in computational modelling.

I would like to thank my batch mates and friends who have assisted me in the progress of my project. My special thanks goes to my beloved parents whose love, affection, patience, blessings, and encouragement helped me in carrying out this work.

SHALABH SINGHAL

M. Tech (Computational Design)

2K16/CDN/05

ABSTRACT

Because of the limited availability of fossil fuels, a major shift can be seen from petrol, diesel vehicles to electric and hydrogen based vehicles in the upcoming times. One of the major chunk of electric vehicles currently in use consists of EMU and high speed trains, which has seen an upsurge in demand in urban cities because of easy, economical, time saving and more comfortable commuting. With increased frequency of service and more and more number of passengers adding on daily, these systems are more prone to fault (or failure) which may lead to loss of life as well as money. So to avoid fault or failure either high preventive maintenance strategies shall be adopted or redundancy shall be increased, both of which leads to an increased cost.

Fault is an unwanted, measurable, non-measurable, monitarable, non-monitarable, susceptible change in characteristics of system (running or at rest), which may or may not result in the failure of the system. Fault diagnosis approach so used involves an interaction of mathematical as well as physical model. Sensors are placed at optimum locations in the system which then interacts with the mathematical functions defining the system, and any inconsistency in the values obtained from output function so observed will be monitored and controlled. Also if a fault occurs, what would be its optimum path of travel is also figured out i.e which components are most likely to fail because of presence of certain fault in certain component.

Using bondgraph, working on the concept of transfer of power (energy is conserved), which is sensitive to any form of spike in energy (either positive or negative), one can fairly predict the possibility of fault and its effect on the consecutive system working online with the help of sensors and ARRs (mathematical function). Thus one can isolate a fault before it becomes critical at subsequent stages. Same can be done in the model of traction system of an EMU which mainly comprises of power supply line, pantograph, transformer, induction motor, gearbox, and wheel. Thus a model is generated on a bondgraph which is simulated and analysed under normal working condition. Also its ARRs are also derived which when compared with the online system (or model) can help in determining the possible faults in the system.

Keywords: Bondgraph modelling, Simulation, Fault analysis, Sensors, EMU**.**

CONTENTS

LIST OF FIGURES

LIST OF TABLES

LIST OF NOMENCLATURE

BG	Bondgraph
I	Inertance
C	Capacitance
R	Resistance
SE	Source of effort
SF	Source of flow
TF	Transformer
GY	Gyrator
Q	Displacement
P	Momentum
t	Time

LIST OF ABBREVIATIONS

kV	Kilo Volt
A	Ampere(current)
s	Seconds
EMU	Electrical Multiple Unit
FDI	Fault Detection and Isolation
ARR	Analytical Redundancy Relation
A.C	Alternating Current
D.C	Direct current

CHAPTER 1

INTRODUCTION

An electric multiple unit or EMU can be understood as coupling of multi-unit train consisting of auto or self-propelled carriages, using electricity (high voltage lines) as the driving power. An EMU requires no separate engine, as electric traction motors (usually 3 phase ac motors) are integrated within one or more of the carriages. Formation of an EMU usually consists of two or more number of semi-permanently coupled carriages, but it should also be noted that electrically powered single-unit or multi coupled single unit rail cars can also be put under the category of EMUs.

1.1 BRIEF ABOUT EMU

There are two meanings of the term "multiple unit" which need to be understood. Two or more number of regular locomotives can be coupled together for greater carrying capacity. In such a case the locomotives are said to be functioning as multiple units, or to be "MU'ed together" (US terminology: "lash-up").

This shall not be muddled with the term electric multiple unit (EMU) or diesel multiple unit (DMU) which is used to refer railcars used for (mostly suburban) train services which usually have multiple hauling units (either electric motors or diesel engines) for each car. i.e., car carrying the passengers also has the motive power, contrary to the normal case where a locomotive hauls the train carrying the passengers and the coaches are not self-propelling. [38]

1.1.1 Types of EMU

The cars that form a complete EMU set can usually be separated by function into four types:

1. Power car

2. Driving car

3. Motor car

4. Trailer car.

Each car can have more than one function, such as a motor-trailer car or power-driving car.

Most of the today's 2-car EMU set up termed as "married pair" units. Though married pair's both the units are typically driving motors, the ancillary equipment (batteries and charging equipment, air compressor and tanks, control equipment, and traction power etc.) are shared between both the cars in the pair. Since neither of them can function without its "partner", such sets are said to be permanently coupled and can only be separated while at maintenance facilities. These married pair units are advantageous because of its cost and weight savings over single-unit cars (halved ancillary equipment used) while allowing cars to be powered at the same time, not like a motor-trailer combo. Each car mostly has only one control cabin, positioned at the exterior end of the pair, saving space and expense compared to a cabin at both ends of each car.

Its major disadvantage comprises of loss of operation under flexible conditions, as EMUs must be a multi-pair of two cars, and a failure on one car could lead to removal of both of them from service. [39]

Fig 1.1: Metro-North Railroad M8 married in New York [40]

Fig 1.2: A First ScotRail Class 380 EMU pairs at Haymarket in Edinburgh, Scotland [40]

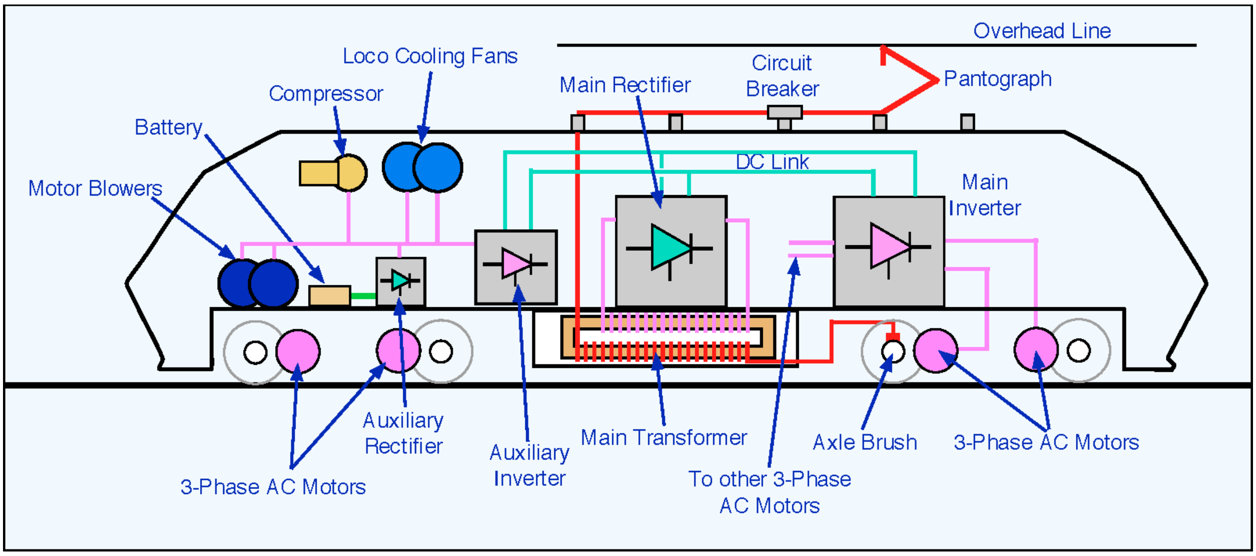

Fig 1.3: Diagram showing an AC electric locomotive, drawing power from an overhead transmission line. The red lines on the diagram indicating single phase AC circuit, the green lines the DC circuits and the purple lines the 3-phase AC circuits. A locomotive using DC traction current is similar, except that there is no single phase AC circuit or transformer. The current passes directly from the pantograph (or shoe) to the main and auxiliary inverters. [38]

1.2 ELECTRIC TRACTION CONTROL

Electric motors are a commoning used to power a train, whether the power or energy requisite to drive the train is obtained from external factors of the train by connecting with an external energy carried by an overhead line or mounted on-board the train as a diesel engine and its fuel.[40] Electric traction and devices are widely used around the globe, especially for routes with heavy traffic, like suburban and urban railways or long distance, high speed lines also need electric traction and devices to achieve the speeds demanded or required for inter-city travel. There are different number of various systems of types of electric traction.

1.2.1 DC and AC Motors

Both DC motors and AC (Alternating Current) motors have the same basic structure but they are different and, for several reasons, the DC motor was in the first place the preferred form of motor for its applications in railway and also most of the systems used it. Today, modern power electronics has developed methodology for the use of AC motors and, for newest equipments designed today, the AC motor is the most preferred type used.

Often, people question the differences between DC and AC motors with respect to their usage in locomotives and multiple-units. In the primeval days of electric traction, at the commencement of this century both types were tested. The setbacks of the technology at that time favoured the use of DC motor. It provided the right amount of torque characteristic required for railway operation and was sensibly simple to control.

Till the early 1980s, power electronics had developed to the stage where the 3-phase AC motor can be used more seriously and more efficiently compared to the DC motor because:

1. They are easier to construct, also they do not require mechanical contacts for their operation (such as brushes) and they are lighter compared to DC motors for same power.
2. Modern electronics permit AC motors to be controlled more effectively to improve both traction and adhesion.
3. Additional advantage of AC motors is that they can also be controlled by a microprocessor to a greater extent and can regenerate current so low at low speeds at which DC regeneration fades quickly.
4. They are easier to maintain and are more robust than DC motors.

The type of motor so discussed is commonly called the Asynchronous Motor and is oftenly referred to as the squirrel cage motor because of its earlier designed form. Both DC and AC motors look similar when looked externally but there are a number of differences in their construction, peculiarly because the DC motor has a commutator and brushes while the AC motor does not have. [38]

1.3 MULTIPLE UNIT CONTROL

It was primitively traced from lift operation around a hundred years ago, multiple unit (MU) control is the mostly used form of train control around the world nowadays.

Originally designed electric locomotives were so made that the motors were controlled right away by the driver. The traction power circuits mounted in the driving cab are passed through a large controller. To decrease or increase power as required driver needed to rotate a handle as required to change the switches in the control circuit. This arrangement's setback was that the driver had to be close to the motors if heavy and long, power-carrying cables were to be fend off.

Although this system also functioned well enough, the wish to get quick turn-rounds on urban streetcar railways, remote control was adopted. The idea behind it was that a set of driver's controls could be kept at each end of the rail/train, only if the motors could be controlled remotely. It would not be necessary to have a locomotive added at the tail of an arriving train to allow it to make the return journey. A cab had to be connected at each end of the train and the driver just need to switch ends to alter direction. Once this idea was recognized, it was appreciated that the motors could now be placed wherever along the length of the train, with as few or as many as requisite to provide the desired performance. With this expansion, instead of housing a few and large motors in a locomotive, more but smaller motors were placed along the train. This is how the concept of trailer cars and motor cars was evolved. Trailer cars are only passenger carrying means of transportation but motor cars are passenger carrying vehicles having motors and their control equipment.

1.4 AC LOCOMOTIVES WITH DC DRIVES

A shortened schematic of a 25 kV AC (Alternating Current) electric locomotive used in the UK in the late 1960s is represented in fig 1.3. The 25 kV AC is gathered by the pantograph mounted on rail-car and passed on to the transformer which is needed to step down the voltage to a level which can be worked with by the traction motors. The level of current which is to be supplied to the motors is precisely controlled by a "tap changer", which switches in more number of sections of the transformer to decrease or increase the voltage passing through to the motors. It functions as the resistance controllers works when used with DC traction, in which the resistance contactors are operated and controlled by camshaft operating under the driver's commands.

Before being sent to the motors, the AC has to be converted to DC by passing it through a rectifier. For the last 30 years and more, rectifiers have been using diodes and their derivatives, the ongoing development of which has directed to the current AC traction systems.

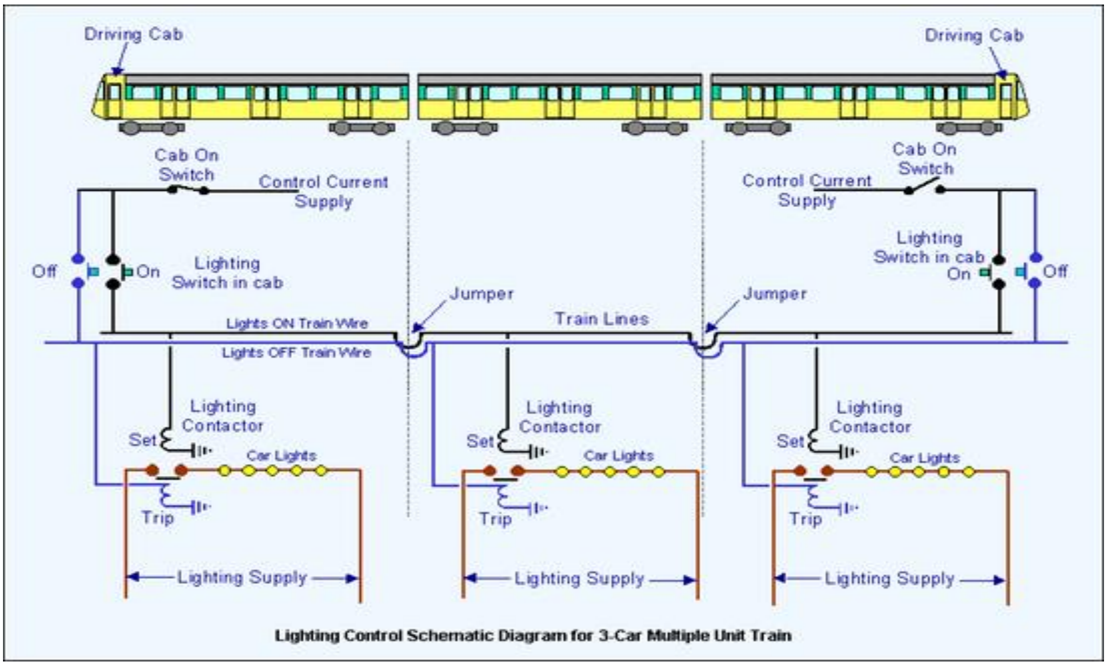

Fig 1.4: Lighting control schematic diagram for 3 car EMU [40]

1.5 AC DRIVE

In AC drive the frequency used to be challenging to control and that is why they were inappropriate for railway functioning, until the dawn of modern electronics, AC motors were almost solely used in applications requiring constant speed. A modern 3-phase traction railway motor is controlled by supplying in three AC currents which network to make the machine to turn. The three phases are suitably provided by an inverter which feeds the three variable voltage, variable frequency (VVVF) motor inputs. The variations of the frequency and voltage are controlled electronically.

The AC motor can be used in either an DC or AC traction supply system. In the case when AC is supplied, the supply line (say 25kV single phase) is fed into a transformer and a secondary winding is for rectifier (AC to DC converter) which generated a DC output of say 1500 - 2000 volts as per the application. It is then passed to the motor converter (inverter) feeding the controlled three phases to the AC traction motors. The connection between the inverter and the rectifier is called the DC link. This typically supplies an output also for the train's auxiliary circuits.

The 3-phase set-up is even simpler when it is applied to a DC traction supply, as it doesn't need a transformer (to step down) or a rectifier. The DC line voltage is applied directly to the inverter, which directly gives the 3-phase motor control.

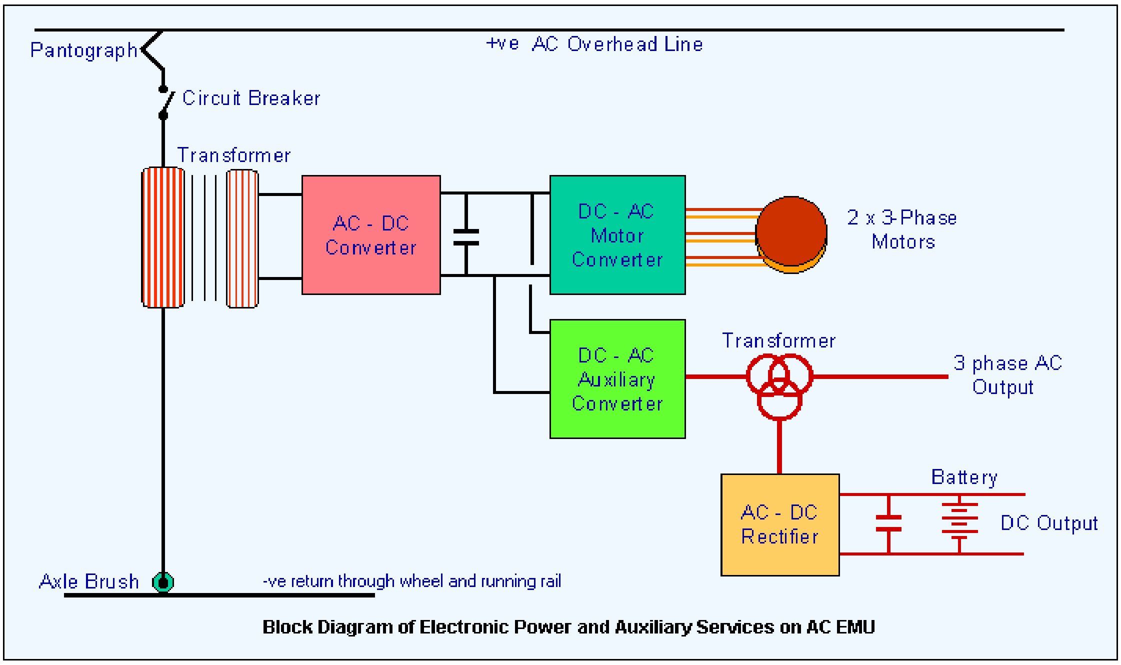

Fig 1.5: Schematic of 25kV traction control system with the 25kV fed into a transformer. A secondary winding is taken off for the AC to DC converter, which produces a DC output to pass to the motor converter, which then provides the controlled three phases to the traction motors. [40]

Control of these systems is not simple but it is all taken care of by microprocessors. The control of the frequency and the voltage pulses has to be harmonized with the motor speed. A set of distinctive buzzing noises are produced because of the changes which occur during this process which usually sound like the "gear changing" of a motor (road) vehicle and it can noticeably be heard when riding on EMU driven by the AC motor car.

1.6 BRIEF ABOUT BONDGRAPH

Bondgraph is a tool based on flow of energy (or power) which describes the system in form of vector states. Bondgraph is both information as well as power oriented. Prof. H.M.Paynter depicted systems in terms of power bonds, connecting the elements (so modelled) of the physical system to the junction structures which were indicators of the constraints. It represents the system in terms of lumped parameters elements of capacitance, resistance, inertance, thus giving us a network structure connected at junction (0s and 1s) (Samantray,2001). Bondgraph also derive the equations of the network structure as vector states and it can be analyzed easily.

1.6.1 Power variables of Bond Graphs

Power interactions of a dynamic system includes Effort and Flow (e.g. force and displacement), which may have different forms in different physical domains. Another feature of Bondgraph includes coupling of these various types of local power variables while designing a single global model.

Table 1.1: Effort and Flow parameters of various systems

Systems	Effort**(e)**	Flow(f)
Mechanical	Force(**F**)	Velocity(v)
	Torque(ج)	Angular velocity(ῳ)
Thermal	Temperature(**T**)	Entropy change rate(ds/dt)
Magnetic	Magneto-motive force($\mathbf{e_m}$)	Magnetic flux($^{\phi}$)
Electrical	Voltage(**V**)	Current(i)
	Pressure(**P**)	Volume change rate(dV/dt)
Chemical	Chemical potential(**µ**)	Mole flow(dN/dt)
	Enthalpy(**h**)	Mass flow(dm/dt)
Hydraulic	Pressure(**P**)	Volume flow rate(dQ/dt)

1.7. BOND GRAPH STANDARD ELEMENTS

In bond graphs, there are four groups of elementary symbols, i.e., three basic one port passive elements, two basic two port elements, two basic active elements and two basic junctions. The basic variables are flow (f), effort (e), time integral of flow i.e. Q and the time integral of effort, represented by P.

R-Elements: The resistor is a 1-port element. Resistors represent dissipation of energy. This is applicable for simple dampers, electrical resistors or dashpots, and other similar inactive elements. For the resistive element the bond graph symbol is shown below. The constitutive correlation between f, e and R is given by:

$$e = R * f$$

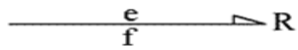

Fig1.6: Bond representation for resistance element

C-Elements: Role of capacitor is to give up and store energy without loss. In the physical terms, a capacitor is a symbolization for devices like springs, gravity tanks, accumulators, torsion bars, and etc. The symbol so used in bondgraph describing constitutive expression for a C-element are shown below:

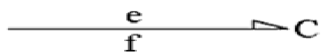

Fig 1.7: Bond representation for Capacitance element

The effort (e) and the displacement (Q) is defined by,

$$e = K \int_{-\infty}^{t} f \text{dt} \qquad Q = \int_{-\infty}^{t} f \text{dt}$$

I-Elements: It is an energy storing port utilized to model inertial effects in mechanical systems and effects of inductance in electrical systems and fluid systems. Inertial element is represented in the bond graph as shown in the figure given below.

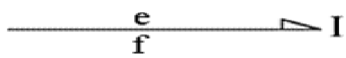

Fig 1.8: Inertance element bond representation

If the mechanics of mass considering as a point is examined, then we would have;

$$P = \int_{-\infty}^{t} e \text{dt}, \qquad f = m^{-1} \int_{-\infty}^{t} e \text{dt}$$

Effort and Flow Sources: Ports which give reaction to the source are also known as active ports. For, example if we climb on a rigid body, our feet feel a reaction with a force or source. Because of this reason, sources are also called as active ports. They are presented by a half arrow directing away from the source (of effort or flow) symbol. The effort source is shown as

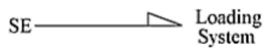

Fig 1.9: Bond representation for source (effort) element

and the source of flow is represented as shown below.

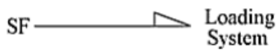

Fig 1.10: Bond representation for source (flow) element

Basic 2-Port Elements-There exist only two types of two port elements, viz. “Transformer” and “Gyrator”. The bond graph symbols used for these 2-port elements are GY and TF, respectively. As the classification suggests, these elements are attached to two bonds.

The Transformer: The transformer in bondgraph can represent an actual electrical transformer or an actual mass less lever, etc. The transformer does not create, destroy or store energy. Energy is conserved in it and it transmits the power factors with proper scaling (up or down) as characterised by the transformer modulus. The concept of a transformer is better understood by an example described here. In this example, we consider a mass less ideal lever. Both bondgraphic and standard nomenclature of a mass-less lever are presented in the image below. It is also assumed that the lever is unbending or rigid, which implements a linear relationship between the power variables at both the extremities of the lever.

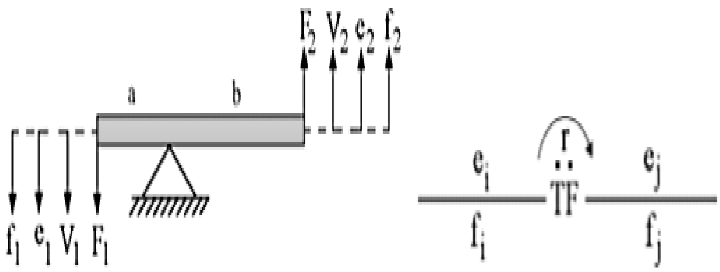

Fig 1.11: Concept of transformer as a lever

The 'r' shown above the transformer symbol represents the modulus or transformation ratio (also called scaling factor) of the transformer, which may be any constant or some expression (like 'b/a'). The small arrow tells the sense of direction in which this modulus is used or transformation is carried out,

$$f_j = r*f_i, \qquad e_j = (1/r)\, e_i.$$

Thus the following expression establishes the conservation of power,

$$e_j\, f_j = e_i\, f_i.$$

The Gyrator: As discussed, a transformer relates effort-to-effort and flow-to-flow. Conversely, a gyrator defines a relationship between effort to flow and flow to effort, but by law of conservation of energy, keeps the power same on the ports. The simplest gyrator one can have intuition of is a mechanical gyroscope, as shown in the figure below [6]

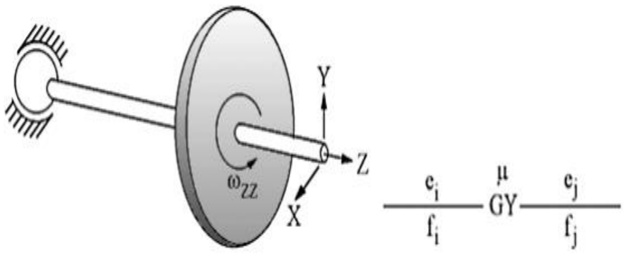

Fig 1.12: Concept of gyrator as a rotating disc

The μ (in Fig-12) above the gyrator represents the gyrator (transformation) modulus, where $\mu = I_{zz}\, w_z$. As it can be observed that modulus is not having a direction sign connected with it. This modulus is always characterized from flow to effort.

$$e_j = \mu\, f_i, \qquad ei = \mu\, f_j.$$

Thus by following expression power is conserved,

$$e_i\, f_i = e_j\, f_j.$$

In the electrical field, an DC motor is ideally represented as a gyrator, where we can co-relate the output torque which is proportional to the current input and the back emf which is proportional to the angular speed of motor. In general, gyrator’s application can be found where power from one energy domain (or field) is transferred to another domain, viz. electrical to magnetic, electrical to rotational, or hydraulic to rotational.

The 3-Port junction elements The name 3-port is a misnomer. Practically, junctions can connect two, three or even more bonds. There are only two types of junctions, the 0 and the 1 junction. They conserve power or energy and are reversible [42]. System topology is represented by them and hence two-port elements and the junctions in a global model (also known as Junction Structure) is power conserving.

1 junction: It is a common flow junction and the sum of effort is zero and the power orientation is same. This junction represents a series connection, like a meeting mass point in a mechanical system (as in an electrical network which represents flow continuity, etc).

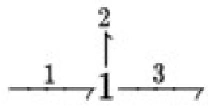

Fig 1.13: Common flow junction

Using the inward power sign convention, the essential relation (for power conservation at the junctions may be written as follows;

$$e1\ f\ 1 + e2\ f\ 2 + e3\ f\ 3 = 0.$$

As 1 junction is a common flow or flow equalizing junction,

$$f\ 1 = f\ 2 = f\ 3.$$

This leads to,

$$e1 = e2 + e3$$

0 junction: The efforts attached on the bonds to a 0-junction are alike and flows algebraically sums to zero. The half-arrow directions determine the signs to be put in the algebraic sum in a bond graph.

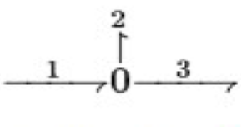

Fig 1.14: Common effort junction

$$e1\ f\ 1 + e2\ f\ 2 + e3\ f\ 3 = 0.$$

As 0 junction is a common effort or effort equalizing junction,

$$e1 = e\ 2 = e\ 3 = e\ 4.$$

This leads to,

$$f1 = f2 + f3.$$

1.8 POWER DIRECTIONS ON THE BONDS

In mechanics, the frame of reference is quite significant. For e.g. a spring-mass system is considered. Now thee displacement of spring is considered with respect to a reference. If both mass and frame of reference is moving, it is noteworthy to assume a set of sign convention i.e. displacement is positive either towards right or left. Also during the course of motion, force and displacement may act in opposite direction., so fixing initial frame of reference is random. So to determine the power direction from/to junction, a convention is defined to allocate positive or negative sign to direction of power. Let's assume a case where effort (or flow) is in same direction of effort of the variables so defined (which makes the system) from junction to element. If it had not been the case, or convention is changed, power's direction won't be reversed, only its sign will change.

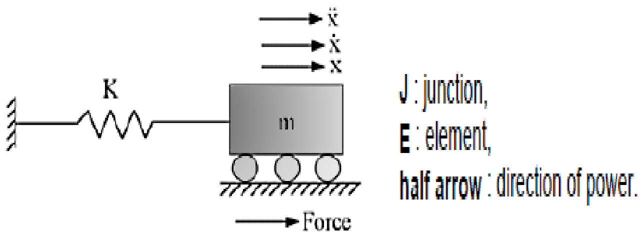

Fig: 1.15 (i)1-D spring-mass system and (ii) power direction

1.9 CAUSALITY

Causality establishes/describes the cause and its effect relationships among the factors of power. In bondgraphs, the outputs and the inputs are described by the causal stroke. Causal stroke tells us in which direction effort signal is traversing (by convention, the end of the bond which have a causal stroke has the effort signal directed towards it). [3]

1.10 RESEARCH OBJECTIVE

The present dissertation work explores the ability of bondgraph to obtain dynamic behaviour of the system under the fault, its detection & its isolation and modelling and generation of ARRS of traction system of an EMU. As Bondgraph offers flexibility in modelling and generation of system equations, a very large traction system is modelled in a modular form (in form of capsules) by creating subsystem models and then joining them together at their interaction port to create an integrated system model. Model is easy modified making it a powerful tool for system synthesis and consolidation of sub-systems. Bondgraph equations normally used generalise displacement and generalized movement as state variables. The bandgap modelling, their simulation and animation is performed using SYMBOLS Sonata, a bondgraph modelling software.

The research's objective is:

1. To create sub-systems of components of traction system and assemble them.
2. To create a dynamic model of a traction system of an EMU by using bondgraph technique and to derive its governing equation.
3. Simulation of the bondgraph model of traction system for variable parameters to obtain the trend for traction force generated on wheels.
4. To generate ARRs for the model with the optimum placement of sensors.
5. To understand the importance of ARR and its significance in determining the fault

1.11 ORGANIZATION OF THESIS

The chapters of the thesis are arranged in the following manner.

Chapter 1 discusses about the basics of EMU and bondgraph modelling. Chapter 2 discusses some literature reviews. Chapter 3 presents the generation of bondgraph models of individual elements of traction system. Chapter 4 presents the basics of ARR and capsules of elements are also generated in this chapter. Chapter 5 presents simulation study. Chapter 6 deals with results and discussion and concludes along with some scope for future wok.

CHAPTER 2

LITERATURE REVIEW

Various researchers have studied and interpreted the physical working models computationally using the bondgraph software. The output parameters obtained in the bondgraph through equations provide a method to study about the dynamics of the system and its input variable effects on the output. Recently researchers have focused on the fault diagnosis and ARR generation of the models being invested and to observe the elements which can be faulty in the system to review and make appropriate suggestions based on the diagnosis. Such papers related to the simulation and fault diagnosis of various applications are discussed below:

(Cho et. al, 1989) [1] have presented a model which aimed at predicting the important dynamics (including those during a shift) quite well when compared to experimental data. A concise mathematical model of power-train dynamics was presented. The model was developed (mostly) based on physical principles and captured the power-train dynamics in the continuous-time domain by the use of eight states and two time-delays. The modeling effort was directed to achieving a reasonable trade-off between simplicity (i.e., low order) and comprehensiveness of the model. A low order model is very desirable not only *to* facilitate the controller design task but also to simplify the real-time implementation of possible "imbedded" model controllers. A great deal of effort was also directed to preserving the generic nature of modeling so that the results of this work can be easily adapted to different types of vehicles. The parameters used represented a typical front wheel-drive mid-size passenger car equipped with a six-cylinder engine and a four-speed automatic transmission. Note that some engine parameters were dimensionally scaled from existing eight-cylinder engine data and well suited for developing a closed-loop power-train controller.

(Staroswiecki. et al, 2000) [3] have presented a united view of model-based approaches for fault detection and isolation (FDI), taking as a guideline the different levels of the knowledge available about the monitored system. Two functions of the FDI process are distinguished, namely alarm generation and alarm interpretation. The numerical and the qualitative model-based approaches are discussed with respect to these two functions. This paper has presented an attempt to integrate both numerical and qualitative model based approaches in a united view of model-based FDI. In order to keep the presentation focused on the FDI design procedure, only very simple mathematical developments have been presented. Many problems have not been addressed at all, or have not been developed. Two functional levels of FDI procedures have been distinguished, namely alarm generation and alarm interpretation. Two levels of the available knowledge are also recognized, the "first one describes what the operator wishes. Faults and perturbations can only be introduced in the second one, this is why it can be used at both the alarm generation and the alarm interpretation levels. On the contrary, alarm-generation procedures based on the operating range model need some extra knowledge for the interpretation task, which can only be qualitatively described.

(Chan et. al, 2002) [5] have presented an overview of the present status of electric and hybrid vehicles worldwide and their state of the art, with emphasis on the engineering philosophy and key technologies. The importance of the integration of technologies electronics, automobile, electric motor drive, controls and energy storage and also the importance of the integration of society strength from government, research institutions, industry, electric power utilities, and transportation authorities were addressed. The key issue of HEV is how to optimize the multiple energy sources to obtain best performance at lower cost. FCEV would have a long term potential to be the conventional vehicle in the future because it is almost zero emission and comparable driving range to ICEV. However, as it is still in the early development stage today, the major setback of FCEV is how to develop low-cost FC, efficient fuel processor, and re-fueling system. A proper engineering philosophy is essential for the guidance of strategic development of EVs.

(Buamama, 2003) [6] have showed that any physical system in its regular operating condition obeys definite mathematical constraints defined by its behavioural model, which essentially is a set of algebrical-differential equations and for the states of the system which can be derived directly from its bond graph model. However, generally in a fault detection and identification model, simultaneous and initial values of states are unknown and such constraints need to be found only in terms of known variables, i.e. the sources and the measurements. Such constraint relations (also termed Analytical Redundancy Relations or ARRs) should always be effective within a certain range of error, while calculated using measured data from the real system. Any inconsistency with measured values in one or more of these constraints is an indicator of fault(s) in some system component. This paper also dealt with a new approach to derive the ARRs from the bond graph model of the system, thus providing a graphical means to optimize the placement of sensors. This approach was illustrated using an example of a Two-Tank system. Suitable repositioning of measurement devices can thus be done over the bond graph model for design of FDI systems.

(Filippini et. al, 2004) [7] have addressed the construction of a four-wheel and a nonlinear vehicle with a dynamic bond graph model and its implementation in the 20sim modeling and simulation environment. Nonlinear effects arising from the coupling of vertical, longitudinal and lateral vehicle dynamics, as well as geometric nonlinearities coming from the suspension system were taken into account. Transmission and a shortened engine models were also included. The modeling task was supported by a multibody representation where the parts were handled as rigid bodies linked by joints. The first step was the 3D-modeling of each, suspension units, chassis, joints and tires as bond graph elements which were also equipped with power ports for physical inter-connection. These 3D-units were later programmed as 20sim bond graph subsystems which when assembled through the power ports allowed for an automated and sectional approach to the construction of the global vehicle model. Simulation experiments corresponding to standard vehicle dynamics tests were presented in order to show the performance of the mode. Numerous elements oriented to multibody systems were also developed thus allowing working with several reference frames, operating with them with the usage of translations and general transformations.

(Staroswiecki et. al, 2004) [9] have developed a bond graph–based model representation mechanism to perform structural level linking of sub-models. The methodology developed is applied to two example systems. Simulation of process faults is used to validate the theoretically obtained fault signatures for a thermo-fluid system in the second example. Different thermo-fluid components have been classified, and their connection syntax to create a valid P&ID has been presented. A formal method for the structural-level linking of different bond graph–based component sub-models has been proposed. Using this level of linking, the structural properties of the process can be determined for control theoretical and fault detection and isolation analysis purposes through variable causality assignments on global bond graph models.

(Medjaher et. al, 2004) [10] have stated an ontology for classifying thermo-fluid process components is presented in this article, along with connection syntax and model validation algorithms. Then the theory for structural analysis is used to design sensor placements for observability and also for component fault detection and isolation. This study also deals with developing a bond graph–based model representation mechanism to perform structural level inking of sub-models. The methodology developed is applied to two example systems. Simulation of process faults is used to validate the theoretically obtained fault signatures for a thermo-fluid system in the second example. Different thermo-fluid components have been classified, and their connection syntax to create a valid P&ID has been presented. A formal method for the structural-level linking of different bond graph–based component sub-models has been proposed. Using this level of linking, the structural properties of the process can be determined for control theoretical and fault detection and isolation analysis purposes through variable causality assignments on global bond graph models.

(Filippini et. al, 2005) [11] have presented the construction of a four-wheel, nonlinear vehicle dynamic bond graph model and it was implemented in the 20sim modeling and simulation environment. Nonlinear effects arising from the coupling of vertical, longitudinal and lateral vehicle dynamics, as well as geometric nonlinearities coming from the suspension system are taken into account. Transmission and (a simplified) engine models are also included. The modeling task is supported by a multibody representation where the parts are handled as rigid bodies linked by joints. The first step was the 3D-modeling of each, suspension units, chassis, tires and joints, as bond graph elements are equipped with power ports for physical inter-connection. This is done with the help of vector or multibond graphs in order to exploit their compactness and simplicity of representation. These 3D-units were later programmed as 20sim bond graph subsystem model which was assembled through the power ports, a flexible approach to the construction of the overall vehicle model. Simulation experiments corresponding to standard vehicle dynamics tests were presented to illustrate the performance of the model. One of the main goals of this paper was the extension of this formalism to include large spatial (3-dimensional) rotations. Several elements oriented to multibody systems were also developed allowing to work with different reference frames, functioning with them through the usage of translations and general transformations. This toolbox works acceptable in the vehicle dynamics prediction and it was successfully applied to another project based on vehicle fault diagnostics.

(Bouamamaa et. al, 2005) [12] have stated an approach to develop and implement model builder software for Fault detection and isolation in the field of thermo-fluid processes. This methodology is based on the analysis of bond graph, structural and functional models. Because of the integration of the functional model as an interface with the human operator, the designer can easily build the thermo-fluid process dynamics models of most technological processes and generate the fault indicators in symbolic format. Instead of developing specific models for specific situations; a generic technique, which can be applied to any thermo-fluid process, is developed in this paper. A methodology based on bond graph analysis and functional modeling has been presented. It aims at developing and implementing a model builder in view of the design of FDI algorithms in the field of thermo-fluid processes. The innovative interest of the presented approach was the use of only one representation (bond graph modeling) for ARRs and dynamic models generation in symbolic format. Furthermore, the methodology was proposed in such a way that, in the implemented software, based on the P&ID of the process plant, the industrial designer can easily (because of integration of the functional tool as interface with the human operator) build the thermo-fluid dynamic and functional models of most technological processes and generate fault indicators. Further work should include chemical processes which will add another class of processes taking into account the material transformation occurring during chemical reactions.

(Sareni1 et. al, 2006) [14] have investigated two simplification methods: the model order reduction algorithm (MORA), depending on the energetic transfers in the systems, and the singular perturbation method (SPM), based on element dynamics. Each method was unswervingly applied on bond graphs. To illustrate its practical application, a railway traction device was chose as an example. The results obtained by both methods are compared and the conditions of use were analyzed. Finally, these two processes have proved their efficiency to reduce the computation time and to simplify the system analysis. By associating the MORA procedure with specific excitation signals, a reduced model was obtained according to the frequency range. These methods were applied on the (linear) mechanical transmission bond graph model of a railway traction system and also on the (non-linear) whole mechanical model. Regarding the mechanical linear bond graph concordant results have been obtained for the SPM and MORA.

(Samantaray et. al, 2006) [15] have obtained ARR from the behavioral model of the system through different procedures of elimination of unknown variables. Bond graph modeling is used in this paper to derive ARR and to obtain the computational model in the case of non-resolvability of equations. A set of sub-graph substitutions in the bond graph model are developed. It is shown that DBG models can be used for online residual computation as well as for offline verification using process data from a database. A method for the coupling of the bond graph model, used to generate the residuals, with a bond graph model, used to describe the process behavior, is presented. The method proposed in this paper enhances the availability of the information for the decision support system by generating all the structurally independent residuals in numerical form. Analysis of the causal paths to the residuals on the diagnostic bond graph model is then used to generate the theoretical fault signature matrix. The model of the residuals, and the fault signature matrix, can be implemented in the real time applications to provide a decision support system including both the fault detection and the isolation capabilities. The diagnostic bond graph model is useful to test the performance of the FDI procedure using both the offline and the simulated data. Simulation studies have been performed on a controlled three-tank system to show, how numerical residuals improve the overall performance of the decision procedure.

(Merzouki et. al, **2007) [16]** have presented fault detection and isolation model based method for backlash phenomenon. The aim of this contribution is to be able to detect then distinguish the undesirable backlash from the useful one inside an electromechanical test bench. The dynamic model of the real system is derived, using the bond graph approach, motivated by the multi-energy domain of such mechatronic system. The innovation interest of the use of the bond graph tool, resides in the exploitation of one language representation for modeling and monitoring the system with presence of mechanical faults. Fault indicators are deduced from the analytical model and used to detect and isolate undesirable backlash fault, including the physical system. Simulation and experimental tests are done on electromechanical test bench which consists of a DC motor carrying a mechanical load, through a reducer part containing a backlash phenomenon. In this work, a model based FDI application on electromechanical system is presented using bond graph approach. At first, the bond graph, in preferred integral causality, is used to model the nonlinear electromechanical system, by combining the multi-physics dynamics. Then, this bond graph tool is used to generate the residuals via the analytical redundancy relations, in order to detect the presence of perturbed backlash phenomenon. Finally, the fault signature matrix is obtained from the residuals expressions, by putting the bond graph model of the system in preferred derivative causality. These fault indicators allowed to monitor the physical system, and to distinguish the undesirable backlash from the useful one by observing the residual responses as shown by the simulation and the experimental results.

(Ghoshal et. al, **2008) [17]** have shown that bicausal BG modelling proves to be a unified approach for sensor placement from the FDI and FTC viewpoint, identification of hardware redundancies for system reconfiguration, generation of fault indicators, estimation of fault parameters for fault accommodation, inversion of systems and actuator sizing for FTC, etc. It is shown that the use of bicausalled BG helps to integrate many of the recently developed advances made in the field of control engineering into development of complex supervision systems. A systematic approach to model-based process supervision with FTC capabilities has been developed by using BG models. The issues of fault detection and isolation, parameter estimation, system inversion, actuator sizing, and finally the design of FTC law have been discussed. We have used bicausality principle and shown that it is indeed a unified approach to handle the aforementioned activities involved in a supervision system. A simple academic example has been used in this paper; however, the developed principles are equally applicable to more complex and general systems.

(Rastogi et. al, 2009) [20] have stated that the dynamic behaviour of a train depends not only on the load but also the mechanical systems, such as dampers, springs etc., which interact with the wheels, the train bogies and body. The effects of railway track imperfections on dynamic behaviour were studied and the effect of the rail irregularity and vehicle speed on ride comfort through numerical simulation were investigated. The model consisted of 17 degree of freedom with wheel set, bogie and car. For assessment of ride comfort Sperling ride index used by Indian Railway was calculated using filtered RMS accelerations. The bond graph modeling and its simulation, was performed using SYMBOLS SHAKTI software, Vertical dynamic was carried out for a typical Indian Railway Vehicle of AC/EMU/T Alternating Current/ Electrical Multiple Unit/ Trailer) type running on broad gauge, a 17 degree of freedom model is used for analysis. Velocity input at all the wheel set was given by considering similar bump irregularity at both WJMS. Vertical acceleration response (output of an input signal) at the car body C.G was measured in the frequency domain. Sperling Ride indices have been found out for the above vehicle. After a comparison of the result so obtained and the standards set by the Indian Railways, the values were found well in the acceptable limit.

(Borutzky, 2009) [21] have demonstrated that some storage elements in a causal bond graph must accept derivative causality and/or if causal paths exist between ports of different resistors, or if the causality assignment procedure leads to closed causal paths in the junction structure, then mathematical models derived from the bond graph take the form of a set of differential algebraic equations (DAEs), which, in general, is semi-explicit and has an index 62, which can be safely solved with freely available numerical codes. However, not only mathematical models in a form suitable for simulation can be derived from causal bond graphs. The determination of inverse system equations is supported by so-called bicausalities.

(Romero et. al, 2009) [22] have suggested a methodology for obtaining the equations corresponding to a mechanism that are necessary for carrying out a kinematic simulation. A simulation of this kind meant obtaining the coordinates dependent on the system according to the movements imposed by the degrees of freedom. In kinematic simulation the movement of the whole set depends exclusively on imposing movement on one or more of the bodies according to the degrees of freedom initially possessed by the mechanism. After analyzing the method of obtaining the required equations for several simple systems, this methodology was applied to the specific case of a front-loader, where in order to move as well as to tilt the bucket, several closed mechanisms were integrated. He also demonstrated the validity of implementing the relevant kinematic equations corresponding to the bucket movement mechanism instead of dynamic equations.

(Ersal et. al, 2009) [23] have established the advantages of the modular approach which include independent creation and reuse of sub-models, hierarchical model structure, ease of adjustment of model complexity, ease of model verification, and ease of handling large systems. A drawback of this approach, however, is that when general-purpose component models are assembled into a system model, the resulting model can be excessively complex for a given application. The component models need to be created for a broad range of applications and, therefore, need to include a lot of detail relevant for that scope.

(Ecole et. al, 2009) [24] have presented fault detection and isolation (FDI) of smart actuators combining the benefits of bond graph modeling with external models. An external model is a generic method which can be used to specify and verify the functional specifications of smart equipment. One drawback of the external model is that it describes the system in terms of functions without taking into account the dynamics of the equipment. The smart actuator, as intelligent equipment, carried out a coherent subset of missions, called USOMs. The logical conditions to move from one USOM to another depend on the services provided by the system's components. In the presence of faults, the alarm decision is taken according to the availability of the elementary system components. In the real industrial supervision tasks, human operators consider the running system in the terms of its functions. Thus, the external model, which describes intelligent equipment from the users' point of view, is used. The bond graph methodology as a graphical modeling language is used. A methodology based on the causal and structural properties of the bond graph models is developed to design FDI algorithms, which can provide the list of faulty components to the USOM. The proposed methodology, incorporating both the external and bond graph models, is applied to a currently acting device (a control valve with a pneumatic servo-motor) in an industrial application.

(Rai et. al, 2009) [25] have presented a new structural approach of analytical redundancy relations generation from linear and linearized bond graphs. The approach considers for the first time the linearized bond graphs enclosing information bonds. And secondly, it uses the graphical algorithm of the transfer function to calculate the analytical redundancy relations directly from the diagnostic bond graph in integral causality. So doing so, the unknown variables elimination procedure is avoided. Due to its simplicity, the proposed approach is well suited for large scale systems. A new structural algorithm for ARRs generation applicable in both linear and linearized bond graphs is presented. The new proposed algorithm of ARRs generation is from one hand graphic in nature, so, it's applicable since the design stage of the technical engineering systems, which allows in turn to perform the features of the FDI system by simple structural analysis, and from other hand, there is no need to calculate the unknown variables, which makes it easy to implement and well suited for large-scale systems. To make this algorithm applicable in both linear and linearized bond graphs, we have presented a modified algorithm of the transfer function, in order to take into account the information bonds in the case of linearized bond graphs.

(Dong et. al, 2010) [26] have proposed a model for research on high-speed railway systems and its automatic control systems. Numerical modeling of high-speed trains in the China and its associate automatic control systems were discussed. Modeling and simulation of train operation systems were analyzed and demonstrated. On the one hand, the model contained several key components such as the train, rail, and air-fluid-soil subsystems. On the other hand, it accounted for the impacts and effects of hybrid coupling of multi-body and multi-state factors.

(Yang et. al, 2010) [27] by analyzing the traction technologies used in existing locomotives and high speed trains, the development and current situation of traction technology were described, and some urgent problems which need to be solved were presented. Firstly, DC motor traction technologies used in Chinese railway were introduced, the development process of DC to AC motor traction locomotives were summarized. Secondly several types of CRH (China Railway High-speed) high speed trains had been compared from the various technical aspects such as main circuit structures, MT ratio, DC link loop etc.

(Yang et. al, 2010) [28] have investigated the path-tracking problem for four-wheel-steering and four-wheel-driving electric vehicles with input constraints, actuator faults, and external resistance. A hybrid fault tolerant and control approach, which chains the linear-quadratic control method to the control Lyapunov function technique, was proposed. It was seen that it not only maintains the vehicle's tracking performance in spite of faults, input constraints, and external resistance but also reduces the cost of the fault tolerant process. A prototype vehicle from the Laboratoire d'Automatique, Génie Informatique et Signal (LAGIS), was used which particularly focused on illustrating the applicability of their approach. It also proposed an optimal hybrid FTC approach with application to the path-tracking control problem for the 4WS4WD Robu-Car vehicle at LAGIS. Several important types of actuator faults were addressed.

(Wang et. al, 2011) [29] have presented an active fault-diagnosis and fault control approach for a four-wheel driven (4WID-independently driven) electric vehicle. An adaptive control-based passive fault-tolerant controller was designed to ensure vehicle system stability and to track the desired vehicle motion when an in-wheel motor/motor driver fault happens. An active fault diagnosis (FD) approach was proposed to explicitly isolate and evaluate the fault. Based on the estimated control gain of the faulty wheel, the control efforts of all the wheels were redistributed to relieve the torque demand on the faulty wheel. An adaptive FTC was employed to maintain the vehicle stability and desired motions when an in-wheel motor/motor driver fault happens and when the active fault diagnosis is being conducted. It was also shown that, despite the small motor control gain estimation errors caused by model inaccuracies, the active fault diagnosis and control gain estimation can provide sufficient information for redistributing the control efforts among the wheels to discourage the use of the faulty wheel motor for avoiding further damages. Simulations with the help of a high-fidelity CarSim full-vehicle was modeled which demonstrated the effectiveness of the proposed and used "active fault diagnosis and fault-tolerant control approaches" in different driving conditions.

(Sia et. al, 2011) [30] have modeled the operative part of a CNC machine using a bond graph approach with optimal placement of sensors in order to achieve a model for an integrated design of supervision. The proposed model allows a conception technically feasible and economically realizable to be integrated into production lines. The generation of analytical redundancy relations can find the FDI (Fault Detection and Isolation) matrix, that optimizes the maintenance function. In this study, we propose a solution for the integrated supervision of this mechatronic system technically feasible and economically realizable to be integrated into production lines, to assist the maintenance operators. The advantage of this method lies in the possibility to have an integrated supervision system adapted for monitoring the parameters of the machine in real time and Direct generation of the FDI matrix signature in real time.

(Kumar et. al, 2014) [31] have stated hunting is a self-excited oscillation caused by the combined action of conicity of the wheels and creep forces acting in the contact plane between wheel and rail. A railway vehicle turns quite unstable after a critical speed and therefore, assessment of the critical speed is vital for comfort and safety of passenger. Kalker’s linear creep formulation had been used for rail-wheel contact forces. The four geometrical parameters namely gauge, cross-level, alignment and vertical profile were used to define tangent track irregularity. Track flexibility was modeled by a one degree of freedom spring mass system. The model was simulated for a given set of nominal parameter values to study the lateral stability behaviour of the wheel set on flexible tangent track. The influence of conicity and wheel radius on stability of railway vehicle was also discussed. A bond graph model of railway wheel set developed for performing wheel stability analysis where it was found that critical hunting velocity is increased and the hunting stability improved at low wheel conicity whereas critical hunting velocity is increased at high nominal rolling radius.

(Merzouki et. al, 2014) [32] have proposed an extension of the causality inversion method by different versions of the same ARR. Fault detection and isolation algorithms are then used to study these faults. The goal is to increase the number of isolable faults. Moreover, structural conditions are given in order to avoid the generation of redundant ARRs. To validate the obtained structural procedure, a fault is imposed in a traction of an omni-directional mobile robot. Extensions of the causality inversion method for diagnosis using the BG modeling tool have been presented in this paper. The proposed technique combines sensor data, in order to generate extra non-redundant ARRs. Structural conditions were proposed so that redundant ARRs are not obtained. To validate our approach, experimental data from a mobile robot, named Robotino was used. The results show that the isolability degree of the system increases.

(Wu et. al, 2015) [33] have proposed a fault prognosis approach via Bayesian network and bond graph modeling techniques to investigate fault propagation mechanism and predict the probabilities of component-level faults accurately for a high-speed railway traction system. Results were validated with a high-speed railway traction simulation system and the effectiveness of the stated approach was demonstrated. Then, a bond graph and Bayesian network based fault prognosis approach was proposed to predict the fault probability of stator and rotor circuit. The fault probabilities of leaf nodes were predicted by joint probability reasoning through Pearl's polytree propagation algorithm.

(Yong Li et. al, 2015) [34] have mentioned how to suppress those motions via an active-suspension method. By exploiting the structural properties of the system model and the triangular control gain, a new control scheme capable of attenuating immeasurable disturbances, compensating modeling uncertainties, and accommodating actuation faults was developed. Compared with most existing methods, the proposed method does not require precise information on the suspension parameters and the detail system model. The controller was tested and validated via computer simulations in the presence of parametric uncertainties and varying operation conditions. An improved dynamic model of active suspension system of the HST which simultaneously accounting for the modeling uncertainties, time-varying and immeasurable system parameters was developed in this paper. By exploiting a structural feature of the control gain matrix, a cost-effective fault-tolerant control scheme was also developed to suppress the lateral vibration and roll vibration of the train body. It was finally shown that the proposed method is not only robust against the modeling uncertainties and disturbances, but also fault tolerant to actuator failures.

(Naim et. al, 2015) [35] have presented the effect of modifying the stator winding in a 1-phase 4-pole starting capacitor induction motor on the table drilling machine into a stator winding of 3-phase 6-pole induction motor on the current, power and rotation of the rotor. Modifications were carried out on the stator winding of a 1-phase induction motor by changing the number of phases, number of poles, type of winding, wire diameter and number of windings per slot. Modifications are carried out on the windings to obtain a 3-phase 6-pole 24-slots induction motor with 200 windings per slot, a wire diameter of 0.5 mm, and a winding type of spiral double layer. In loading test on the induction motor at table drill machine the current average decreased by 3,56 Ampere or 81,6 %, a power average decreased by 191,4 Watt or 40,06 %, and rotor rotation decreased by 499,7 rpm or 33,75 %.

(Varga et. al, 2015) [36] have extended extends the analytical redundancy techniques, well developed for linear systems, to FDI in non-linear dynamic systems modeled by polynomial differential algebraic equations. The residual evaluation form is developed for sensor, actuator and process component faults. Robust structured analytical redundancy relations can be designed for algebraic dynamic systems, thus extending the parity-space approach. Further extensions to rational systems and algebraic discrete-time systems can be done. It should also be noticed that non-linear systems that are not algebraic can be transformed into algebraic systems, especially in cases where the non-linearities appear through sines, cosines, logarithms, or exponentials. Detectability issues have been discussed, and the definition of D-detectability has been introduced.

(Khemliche et. al, 2016) [37] have presented Bond Graph modeling, simulation and monitoring of ultrasonic linear motors. Only the vibration of piezoelectric ceramics and stator will be taken into account. Contact problems between stator and rotor are not treated here. So, standing and travelling waves will be briefly presented since the majority of the motors use another wave type to generate the stator vibration and thus obtain the elliptic trajectory of the points on the surface of the stator in the first time. The simulations of an ultrasonic linear motor are then performed and experimental results on a prototype built at the laboratory are presented. Finally, validation of the Bond Graph method for modeling is carried out, comparing both simulation and experiment results. This paper describes the application of the FDI approach to an electrical system. The main contribution of the work presented in this paper consists in the description of Bond Graph modeling of travelling wave ultrasonic motor, and simulation characteristics. The modeling of the travelling wave ultrasonic motor and its simulation is an important task to understand the principle of operation and its dynamic behaviour.

CHAPTER 3

COMPUTATIONAL MODELS OF ELEMENTS OF RAILWAY TRACTION SYSTEM

Components of railway traction system are modeled on Bondgraph using SYMBOLS Sonata. Motor so considered is a 3 phase ac induction motor which is connected to an input AC source which has been step down using a transformer. After it, a gearbox is connected to transfer the torque as per the gear ratio.

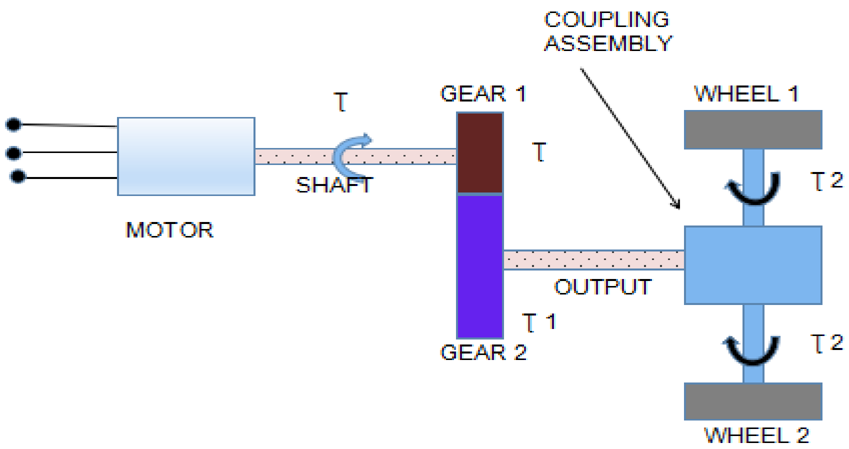

Fig 3.1: Physical Model of Traction System

3.1 MOTOR

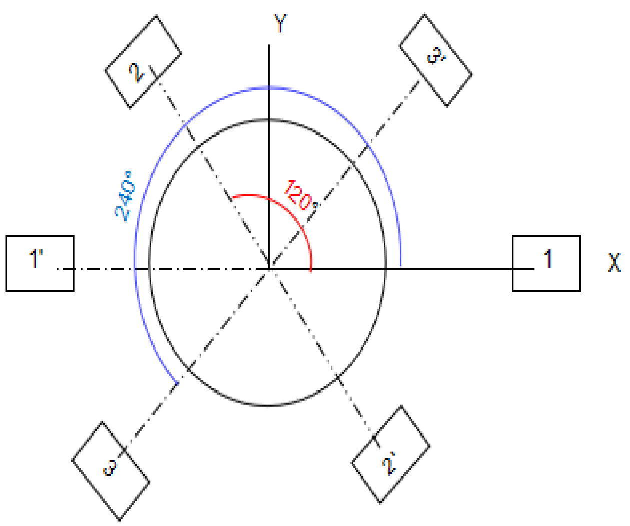

Fig 3.2: Physical model of 3 phase ac induction motor

As it is a 3-phase AC motor, it is provided with 3 inputs i.e. Source of effort (SE). I23, I27, I15 represents stator mass which is one of the input parameter. C5 & C40 represents core capacitance. I18 and I37 is used for rotor mass, also an input parameter, whereas I44 is the load inertia (polar), on which the output torque is measured.

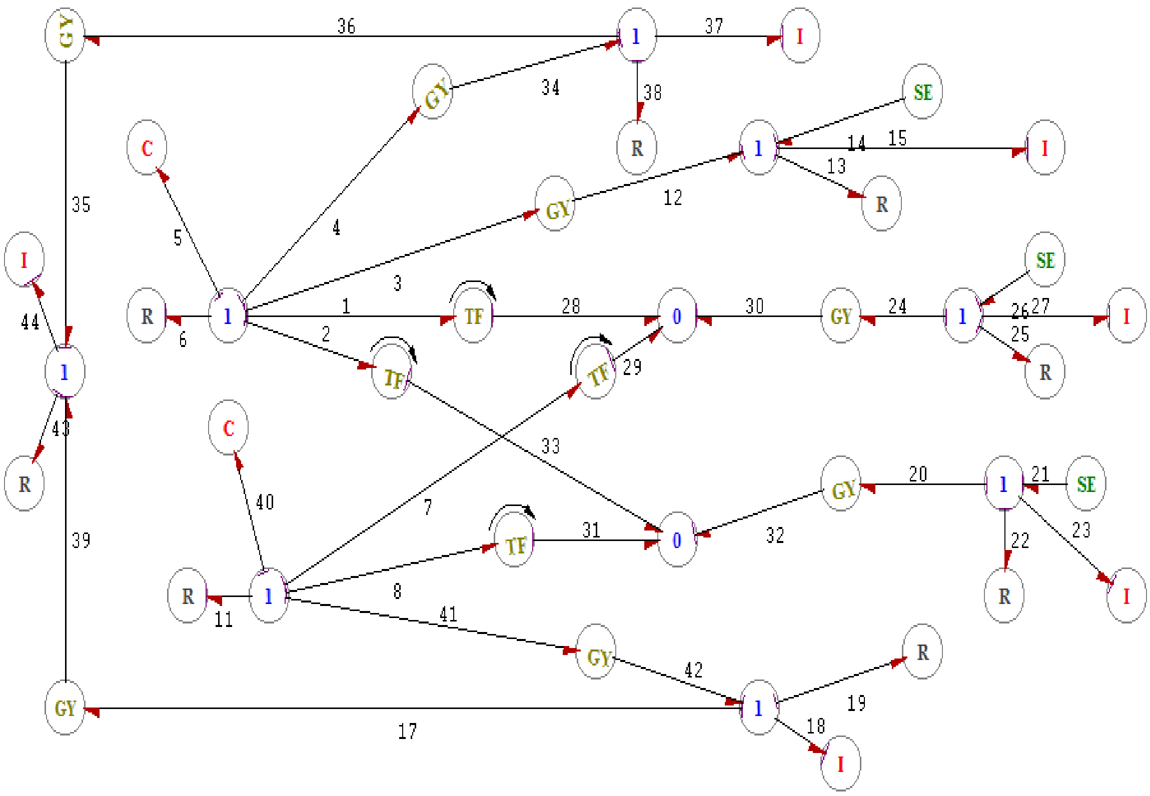

Fig 3.3: Bondgraph model of 3 phase AC induction motor

3.2 GEARBOX

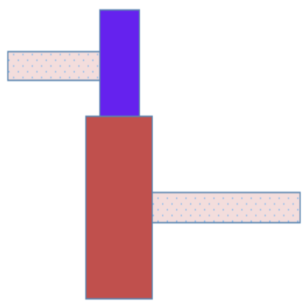

Fig 3.4: Physical Model of Gearbox

Gearbox so designed consists of just one transformation with a transformation ratio of 7.2. SE represents the input torque whereas both I represent the polar moment of inertia of gears.

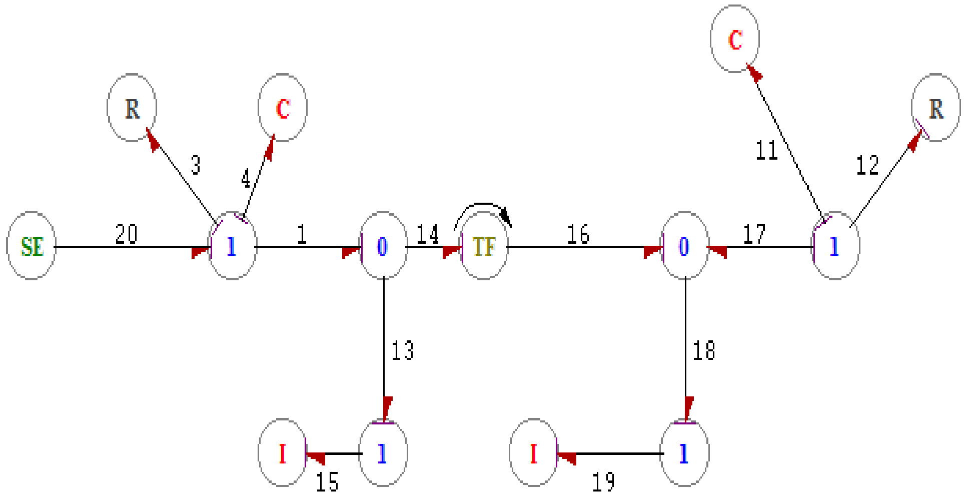

Fig 3.5: Bondgraph model of Gearbox

3.3 BOGIE

Bogie so designed is a system of various lumped masses which is attached on the wheels.

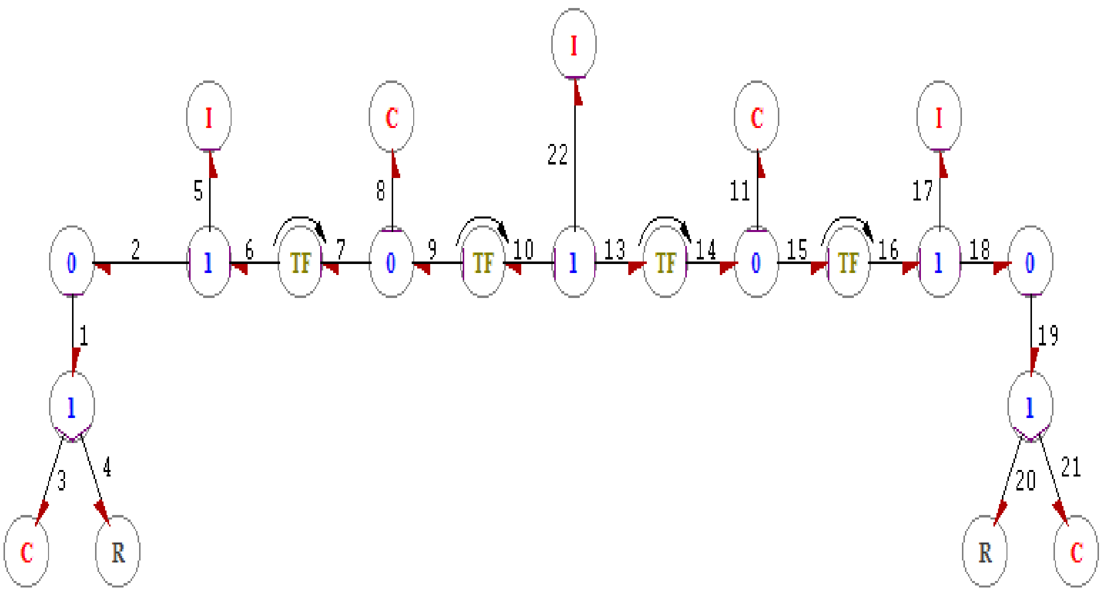

Fig 3.6: Bondgraph model of bogie

3.4 WHEEL

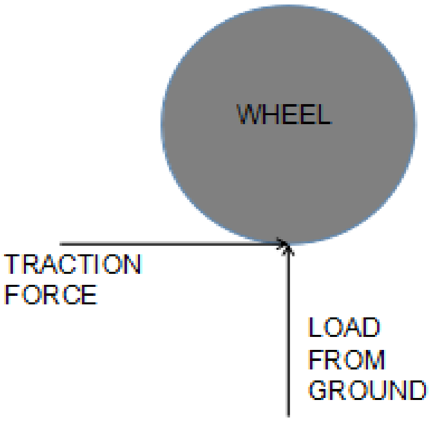

Fig 3.7: Physical model of wheel

SE represents the input torque on the wheel from the gearbox which is transformed to force by using a transformation ratio of 1/r, where r is radius of the wheel and I is the mass of wheel.

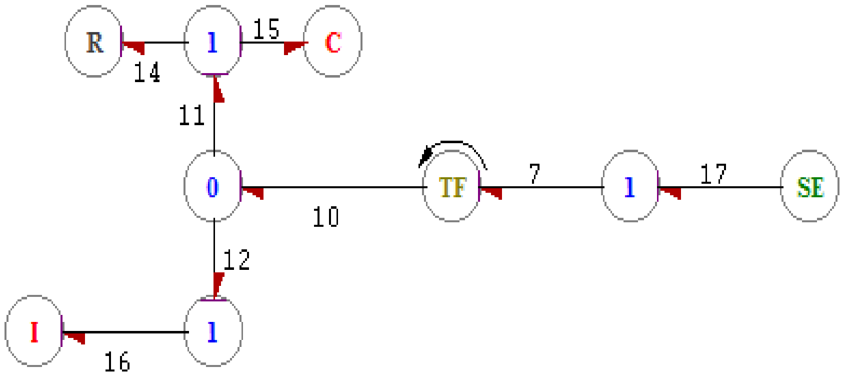

Fig 3.8: Bondgraph model of Wheel

3.5 ASSEMBLED CAPSULES

Initially a 3-phase source voltage is constructed which delivers power to motor which is further dismantles into two components i.e. electrical and mechanical. Motor thus transmits torque to gearbox which further delivers it to wheel while interacting with the load of bogie.

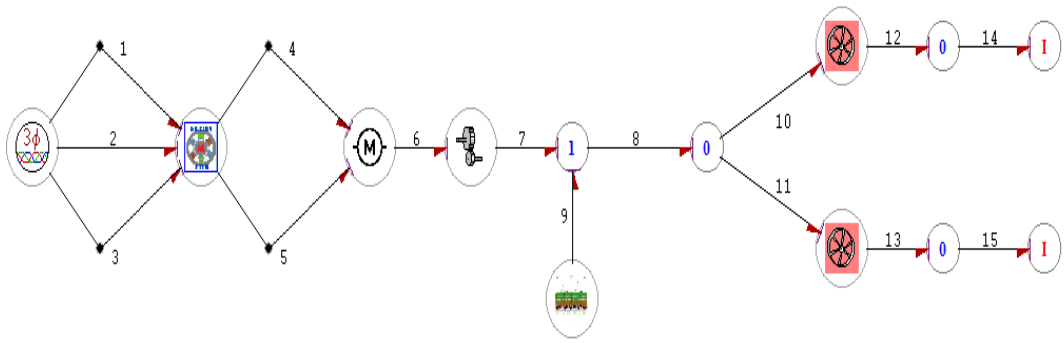

Fig 3.9: Assembled model of traction system

CHAPTER 4

ARR, FDI AND CAPSULE GENERATION

4.1 INTRODUCTION (FDI)

In order for recovery from a fault, two tasks are performed by supervision system- one is FDI and other is decision making. Some special set of tools and methods are devised by supervision systems for normal situation working and working with failures or disturbances. Monitoring level or level of monitoring which detects the fault, if present, and also determines whether the process is working normally or not. It also determines that associated tools responsible for diagnosing are executed after an anomaly or abnormal state of process is detected. If the system's parameters or constraints change because of a fault, fault is accommodated. Fault so accommodated is a process of fault accommodation (F.A). It is performed with the help of Fault Tolerant and Control or reconfiguring the system. FTC's main objective is controlling the system when system is running under actual parameters. In reconfiguration, system with actual fault is exchanged with working one.

FTC approach has two further classifications- one is active (robust) approach and other is passive (adaptive) approach. Active FTC involves diagnosing the faults and redesigning the controller for accommodating faults. For FDI, a model needs to be created which requires mathematical model.

In Bondgraph model, junctions have two laws- strong, representing equality constraints and weak, describing algebraic constant. Each source element brings an input constraint and each passive element like capacitance and resistance defines constitutive relation. Model has equal number of unknowns and constraint relations. Except for cases of causality, each power variable has its derived equations in terms of state vectors. For FDI, some of the outputs are available to us with the help of sensors. Thus, these outputs add to number of equations of the model, increasing the redundancy in equations which lead to formation of ARRs. Number of ARRs that must be generated equals the number of sensors incorporated in the model.

When faults are detected in the system, a robust decision procedure is required so as to generate alarm and eliminate the chances of misdetection of states/residuals. Though it is preferred to go for partial decoupling of residuals from modeling, but it is also possible to go for perfect decoupling if the number of parameters are few.

Passive approach aims at achieving robustness in FDI methods at decision-making stage itself. Here, adaptive methods are adopted once the uncertainties effect the residuals. Each residual, r_i, is tested by a decision variable K (r_1, r_2, ….. r_n) which generates a coherence vector, C, against adaptive threshold, d_i (which may be function of some parameters). C_i is determined by

$$Ci = \begin{cases} 0 \text{ if } r_i \text{ is bounded by } \delta_i; \\ 1 \text{ otherwise:} \end{cases}$$

A fault signature matrix (FSM) describes the sensitivities of residual with respect to various faults. Detection of fault is done by the help of residual, when it violates its threshold. Thus the elements of FSM define the relation of i^{th} ARR with j^{th} component.

Causal bondgraph model helps in determining the FSM, Structured Residual (or a set of residuals) responds to only one fault whereas in diagonal residual multiple faults are isolated. Each set of ARR represent a particular causality in BG model.

4.2 ALGORITHM FOR CONSTRUCTION OF FSM

1. Each Sensor imparts information about both flow and effort to thr junction through a strong bond, which shall be bicausaled.
2. Terminating nodes which receives information about both effort and flow, helps in determining ARR in a non-rigid way.
3. Sensor with causality to a terminated node are identified which give fault signature associated with an ARR.

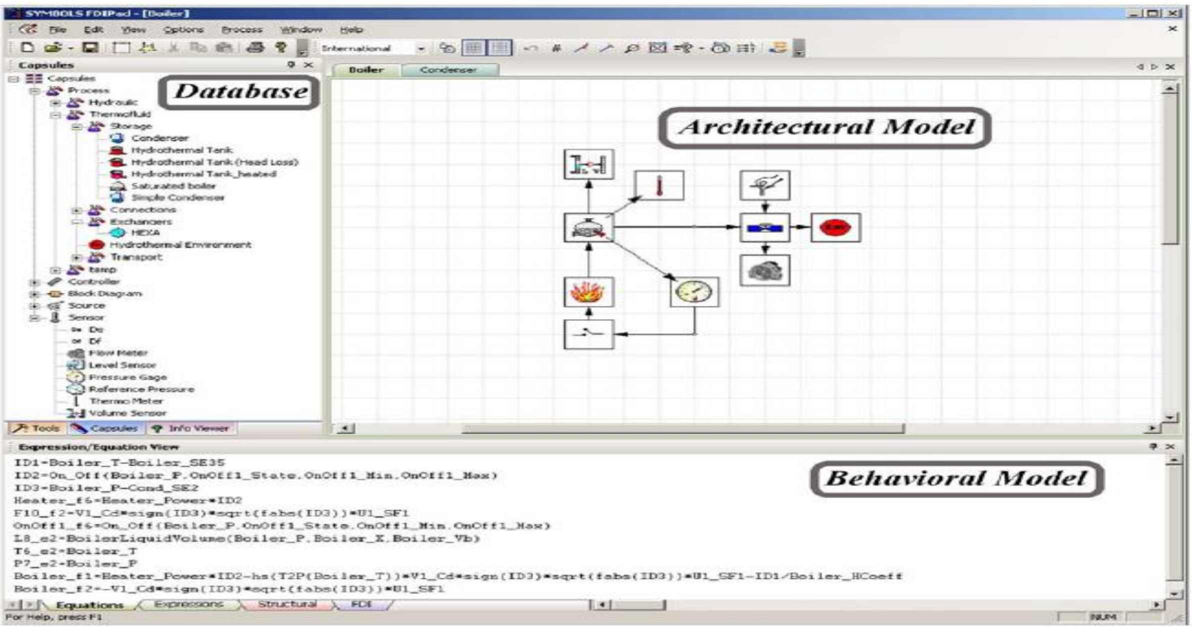

Fig 4.1: Software interface for model builder and ARRs generation

4.3. BRIEF ABOUT ANALYTICAL REDUNDANCY RELATIONS (ARR)

An **ARR** is a relationship between a set of known process variables, *Se* and *Sf*, the sensor measurements (*De* and *Df*), etc. Residual represents the difference in the value of constraint between measured one and one obtained from mathematical model. A residual, R can be written as:

$$R = f\,(De, Df, Se, Sf, MSe, MSf, u, \mathrm{q}) = f\,(K) = 0,$$

where *f* is the constraining function.

For a system with *n* structurally independent residuals;

$$R_i = f_i\,(K_i),$$

where $i=1 \ldots n$ and $K_i$is the set of known variables in the argument of function f_i; the following property is satisfied:

$$K_i > \neq K_j \forall i \neq j \text{ , where } i, j = 1 \ldots n.$$

Residuals are kept equal to zero for ideal cases but not in practical system where there are noises in sensors. Evaluation of ARR detects faults and generate a coherence vector, $C=[c_1,c_2,...,c_n]$, whose elements, $c_i(i=1...n)$, are determined from a decision procedure, Θ, which generates the alarm conditions. Objective of decision procedure so developed is to avoid misdetection of fault and preventing to raise false alarms, each residual R is tested against a threshold.

Detection of fault is obtained by observing coherence vector, C which when not equal to zero or at least one of its element is not zero. FSM defines the dependence of particular element in that ARR.A variable is monitorable ($M_b = 1$) if it appears in at least one residual. Thus if fault is monitorable and its signature is unique, it can be isolated.

Any finite dimensional graph can be specified with three sub-graph:
An over-constrained subsystem, where variables must agree with more than the number of constraints, a just-constrained subsystem, where variables are equal to constraints, an under-constrained subsystem, where variables are more than number of constraints. ARR is obtained with help of over-constrained subsystem.

Bond graph modelling used for fault detection and isolation, must satisfy the following three conditions for residual based diagnosis:
Assumption: A single fault hypothesis is considered.

1. All the storage elements in the behavioural bond graph model are in integral causality.
2. All the states of the system are observable in the given operating range.
3. When preferred derivative causality is assigned to storage elements in the bond graph model, there are no causal loops involving two or more storage elements.

4.3.1 Disadvantages of classical ARR derivation method

1. Currently, the derivation of ARR with the help of BG is not well structured.
2. There structural independence is checked after residuals are generated using laws of conservation at junctions.

If the difference between measured value from a sensor and calculated value from expression is zero than a residual is generated which is observed by a virtual sensor in BG model.It is as shown in Fig. 4(b).

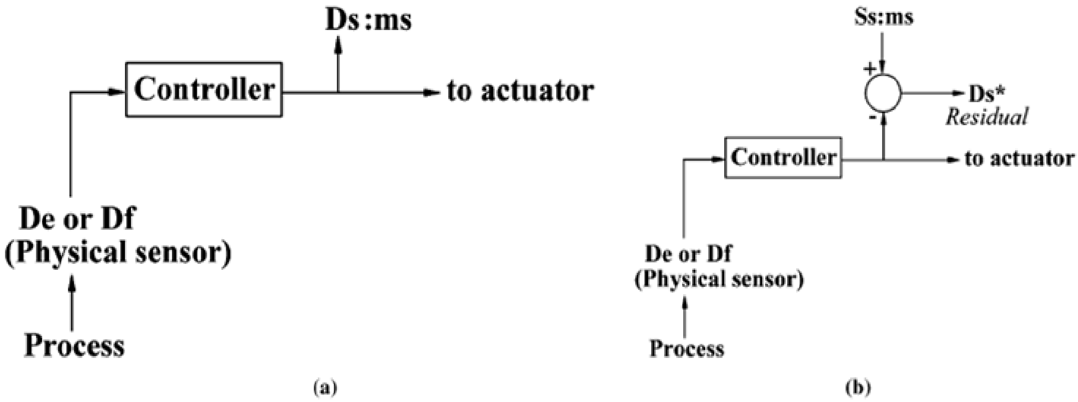

Fig: 4.2 (a) Signal Sensor, Ds (b) Corresponding substitution and residual sensor

For the sensors, whose causalities have been inverted, residuals are observed in their dual sensors; whereas for the sensors, whose causalities have not been inverted, residuals are observed in similar sensors. The residuals for the controllers are simple comparisons of the measured outputs and the predicted outputs. For this purpose, each signal sensor, Ds, is always converted to a signal source, Ss, and the residual is obtained using simple comparison, as shown in fig 4.2.

4.4 DERIVATION OF ANALYTICAL REDUNDANCY RELATIONS (ARRs)

All the storage elements in the bond graph model are assigned derivative causality. The number of residuals is equal to the number of actual sensors. In residuals, sensors with inverted causality at least one causal path is there as compared to other sensors with inverted causalty. If such sensors have same or identical causal paths, they become mutually redundant. Sensors without inversion, residual sensors have the causal path from those sensor measurements. This proves that all the virtual residual sensors have distinct signatures, i.e. residuals obtained are always structurally independent. [43]

Setback of such a method is that sensitivity or response of residuals is not represented to various faults. Residual's effect is easy to analyze in the form of equation. But if it is in numerical form, sensitivities for residuals is taken care through simulations. The coherence vector is created in response of the sensitivity of residual to different faults. This leads to development of FSM by stacking coherence vectors. The practical fault signature matrix refines the theoretical fault signature matrix by removing some influences (replacing 1_s by 0_s).

4.5 DESCRIPTION OF A CAPSULE

A capsule as the name suggests, is a small packet or concise representation of a bondgraph so as to represent a larger bondgraph with an icon to be further used in a bigger model or model with large number of sub-systems. Information of its equations, internal model, mathematical relations and external ports is contained in capsule. A capsule which is designed properly, is precisely complete within itself, self-explanatory, and concise as per the depth of implementation. 'SYMBOLS SONATA' also comprises of Generic capsules, which are given beforehand/inbuilt so as to facilitate modeller in his modeling. They are complete sets of all the causal relations, so required, of the commonly used components. In 'SYMBOLS SONATA', a layout of the major system, including sub systems, represented as a block diagram, can be constructed with the help capsules. When block diagram is made using capsules, they are linked with the help of causality and power strokes which makes the validation by the software easier. Capsules are clustered as per their area of application e.g. 3 phase induction motor is kept under electrical group, wheel, gearbox is placed in mechanical group.

A great deal of customization is presented to the modelers so as to creation of their own personal capsule, different for different users. To build a capsule, first and foremost step is to identify the component and how it is interacting with the external system also known as host model. If a capsule has external output or input or both, it is considered as open system. A closed system (or capsule) doesn’t need external input or output. Generally, most of the capsules are open systems, so as to interact with the main system and also to define the type of interaction (e.g. flow is given to the system or effort). Four types of glue port elements are used to link the current capsule or bondgraph sub-system to the System. These glue ports are viz. EI (effort input), EO (effort output), FI (flow input) and FO (flow output) ports. These ports acts as a broken bond, one of which is acting on system and other on the universe. Input ports infer power is directed into the sub-system while the output ports represent the opposite. Consider an abstract sub-model for a 3 phase 6 pole ac induction motor.

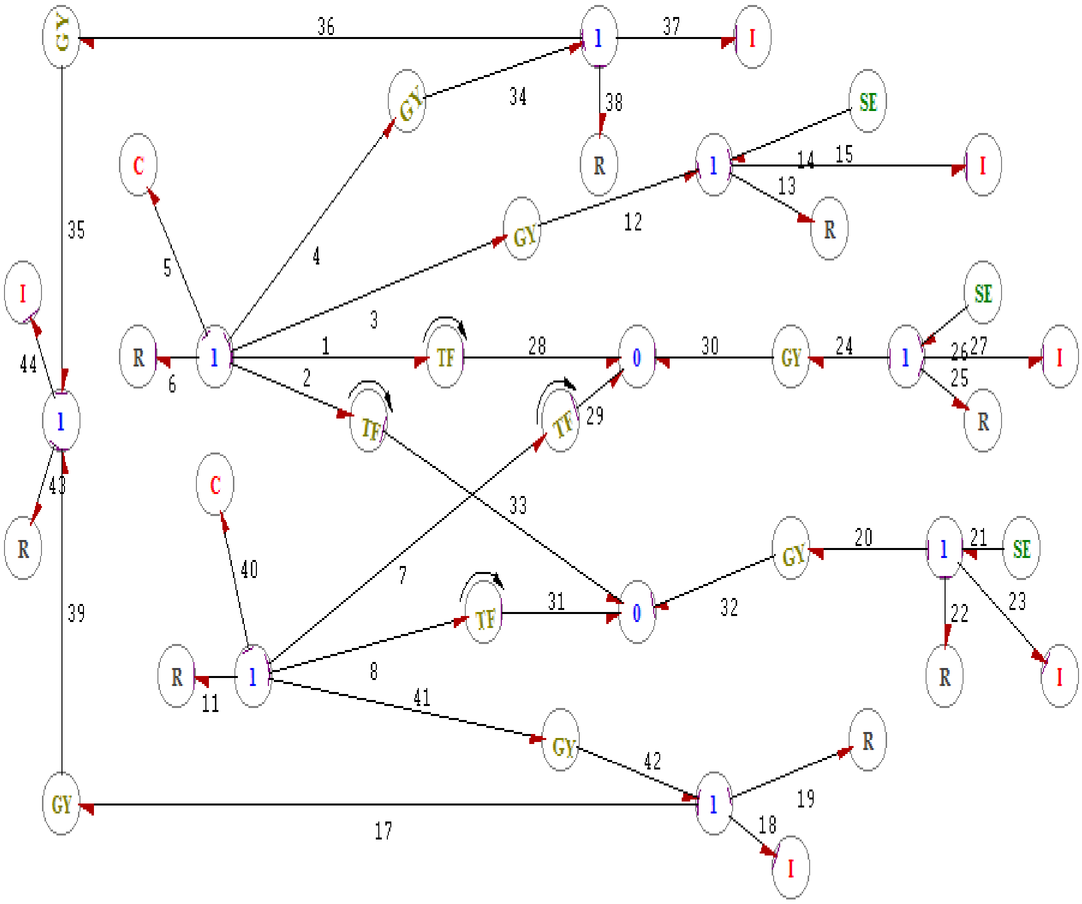

Fig 4.3: Bondgraph model of a 3phase 6 pole AC induction motor.

This model has been separated into two parts i.e electrical (consisting of input source voltage and stator part) and mechanical (consist rotor part and output shaft). In the upcoming pages, electrical part of motor is considered as an example in development of capsule.

4.6 GENERATION OF CAPSULES

<u>Step 1- Defining the external glue ports with descriptive information.</u>

The glue port on the right can be termed as 'Supply Voltage'. The top and bottom port can be named as the 'output from stator'. These comments can be entered using available tool to name ports.

- Represents effort input to the system under consideration.

- Represents effort output from the system under consideration.

Step 2- Suitable annotation and nomenclature of input parameters.

All parameters which are to be made input are defined with the help of comments. For example, here number of rotor coils is represented by N_r, N_s represents the number of stator coils.

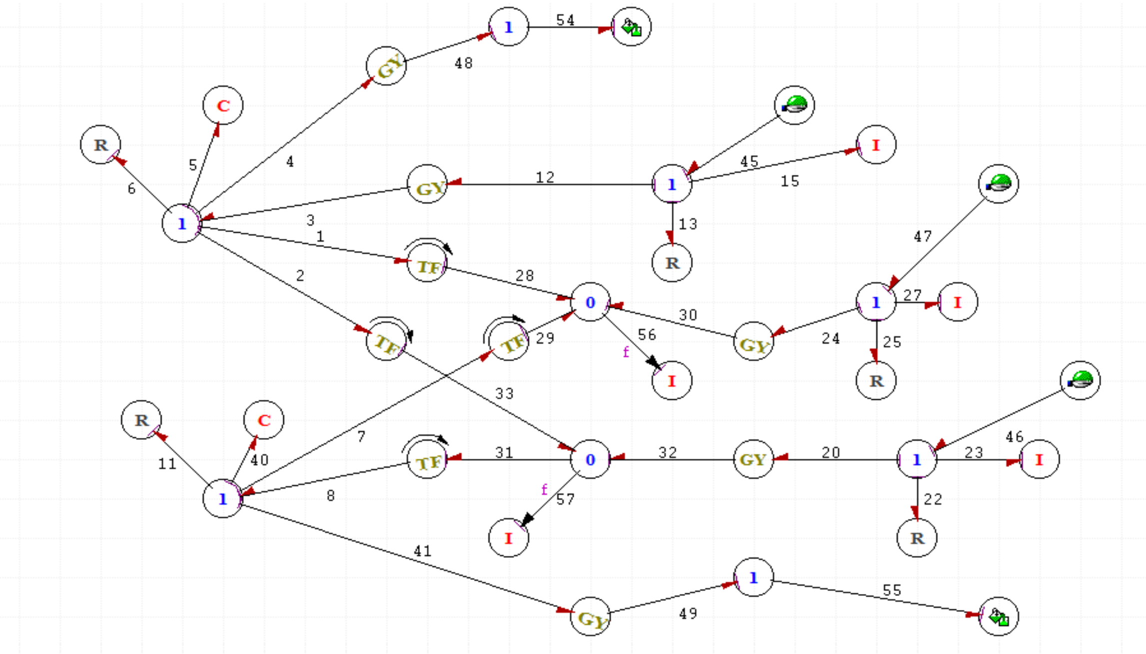

Fig 4.4: Capsule of electrical part of motor

Step 3- Explanation of States in requisite system terms.

Generally, any system in bondgraph has two states connected with it, i.e. Q and P, where Q is for displacement and P represents momentum and derivative of P gives force (or effort). And these states can be defined with respect to the element under consideration (I, C or R) like P27 can be named as momentum of stator.

Step 4- Assignment of a proper icon and placing under a defined group.

Capsule icon is created by the icon editor. Then, the sub-model capsule is placed in any of the capsule group defined earlier; in this case this can be set to the Electrical capsule's group. Once the capsule is created, it can be used in any other model as well. The capsule can be modified as per the need of modeler when required.

4.7 OTHER CAPSULES GENERATION

Other Capsules which were generated as well are:

4.7.1 Mechanical part of motor (rotor and output)   Represented by icon

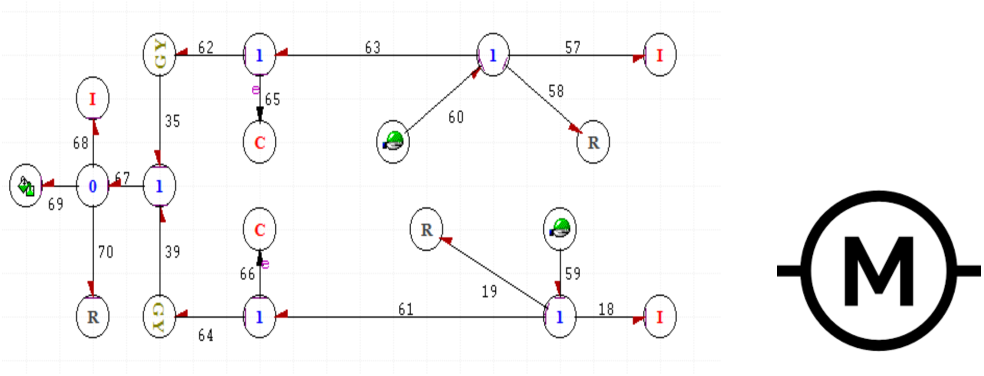

Fig4.5: Capsule for Mechanical part of motor and its icon

4.7.2 Gearbox   Represented by icon

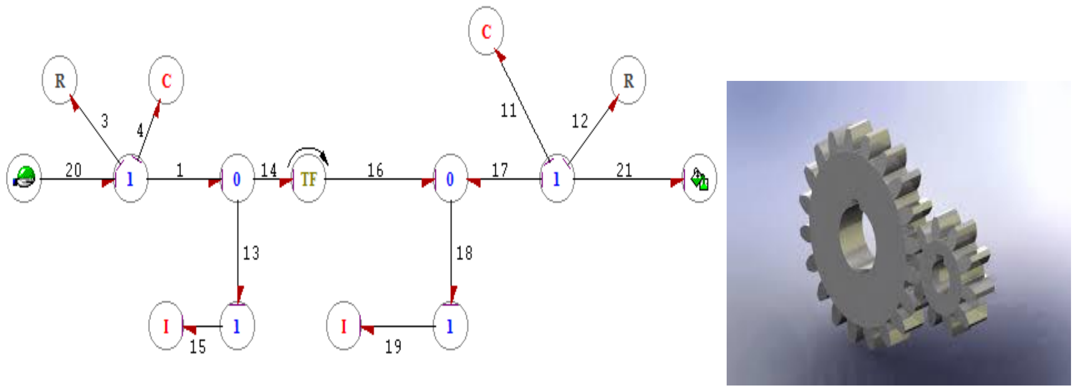

Fig 4.6: Capsule for Gearbox and its icon

4.7.3 Wheel   Represented by icon

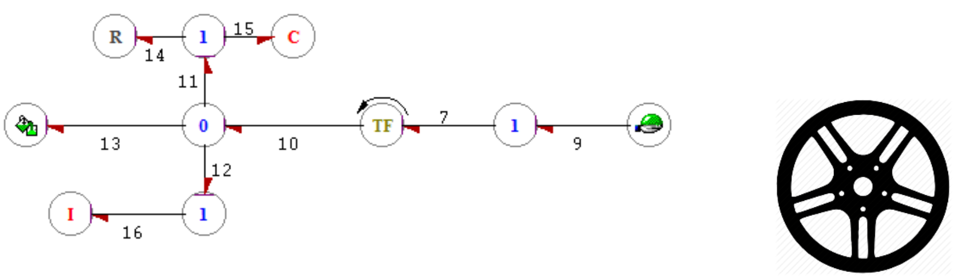

Fig 4.7: Capsule for Wheel and its icon

4.7.4 Bogie

Represented by icon

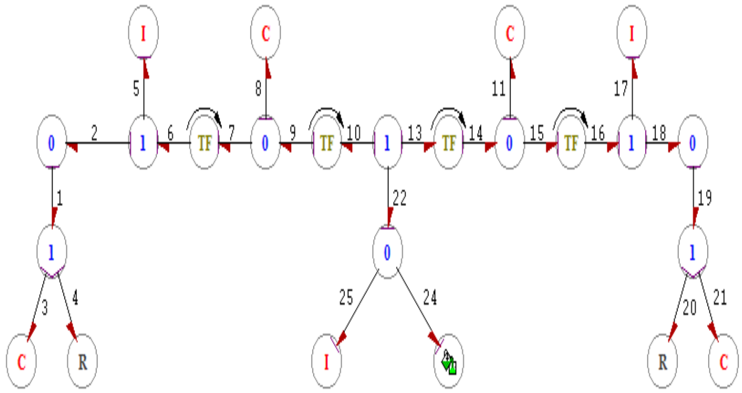

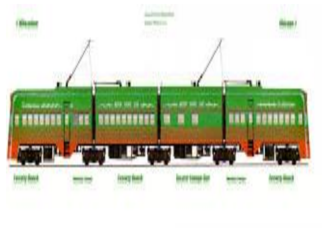

Fig 4.8: Capsule for bogie and its icon

4.8 DERIVING NEW CAPSULES AND MULTIPLE INHERITANCE

Newer capsules may be created from scratch or derived from existing ones. A capsule that uses multiple inheritance is created using several other capsules and/or multiple use of one or more capsules. For instance, the sub-model of an electrical part of a 3-phase ac induction motor where causality at core is removed can be derived from the earlier model with suitable modifications of parameter expressions as shown below.

Expression/Equation View

Variable	Assignment
_cos120 (double)	_cos120=-0.5;
_sin120 (double)	_sin120=0.866;
_sin240 (double)	_sin240=-0.866;
_cos240 (double)	_cos240=-0.5;
_Ns (double)	_Ns=_Numberofstatorcoils;
_I23 (double)	_I23=_statormass;
_I27 (double)	_I27=_statormass;
_Nr (double)	_Nr=_Numberofrotorcoils;
_I15 (double)	_I15=_statormass;
_C40 (double)	_C40=_Kcore;
_Numberofrotorcoils (double)	

Fig 4.9: Expressions of derived capsule

The equations derived for this capsule are shown below. They include unlinked variable expressions for all internal capsules with appropriate prefix. The underscore (_) leaves scope for further extensions.

```
Expression/Equation View
_f15=_P15/_I15
_e40=1/_C40*_Q40
_e3=_Ns*_P15/_I15
_e32=_Ns*_P23/_I23
_e30=_Ns*_P27/_I27
_e25=_R25*_P27/_I27
_e22=_R22*_P23/_I23
_e13=_R13*_P15/_I15
_e1=_cos120*_Ns*_P27/_I27
_e7=_sin120*_Ns*_P27/_I27
_e2=_cos240*_Ns*_P23/_I23
_e8=_sin240*_Ns*_P23/_I23
_f28=_cos120*_f6
_f29=_sin120*_f11
_f33=_cos240*_f6
```

Fig 4.10: Equations of derived capsule

CHAPTER 5

SIMULATION STUDY

The obtained results are shown in this chapter in chronological order as per the block diagram of the model. First angular momentum and torque on output shaft of motor is shown which then acts as an input to gearbox. Second, interaction of bogie with wheel (its self-load and force transferred to it via wheels) is presented. Lastly traction force generated by wheel and momentum of wheel is shown along with their comparison on a single plot.

Some input parameters are considered as per IRFCA guidelines, which could be implemented easily. Where material of the component is known, its elastic modulus is considered. All the resistances used in modelling are kept below 0.5, considering very less dissipation of energy or system's very less resistance to input behavior. Rest other parameters were considered unity.

In table 5.1, the simulation parameters used for simulation of motor, gearbox, bogie and wheel has been shown. These parameters are used to populate the state space representation of the bondgraph model.

Table 5.1 Parameter values for simulation

Parameters	**Value**
3 phase induction motor	
Voltage	240V
Stator Resistance	0.300Ω
Rotor Resistance	0.250Ω
Core Inductance	0.092H
Rotor inertia(polar)	0.091Kgm^2
Number of stator coils	200
Number of rotor coils	1
Gearbox	
Gear Ratio	7.2

Wheel	
Radius of wheel	0.45m
Mass of wheel	800Kg
Modulus of elasticity	200 GPa
Bogie	
Load	100Kg

Graphs so generated may be altered as per the input variables and their degree of accuracy. It is the trend which is of main concern here and time under which system achieves stability under dynamic (or running) conditions.

5.1 MOTOR SHAFT MOMENTUM V/S TIME:

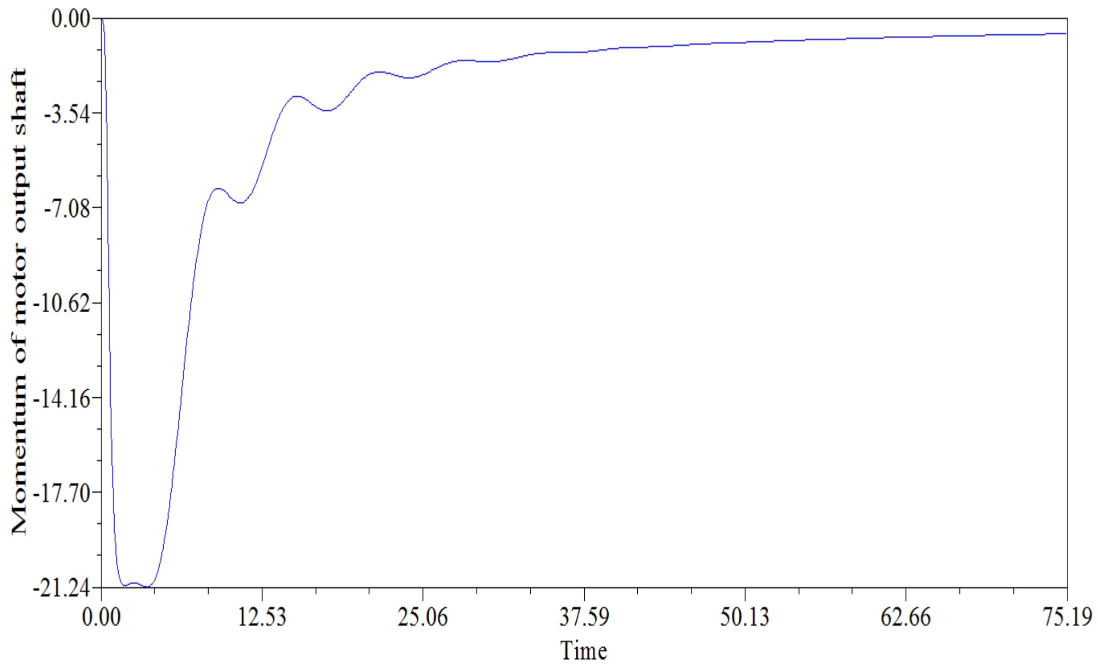

Fig 5.1: Momentum of output shaft of motor v/s time

Momentum of output shaft of rotor is shown in fig 5.1. This figure shows that negative but high value indicated a change in momentum because of starting torque required to compensate for the high starting load. Once the system attains its dynamic characteristics, it tends to become stable at very low value of momentum at 46.02s.

5.2 OUTPUT TORQUE OF MOTOR:

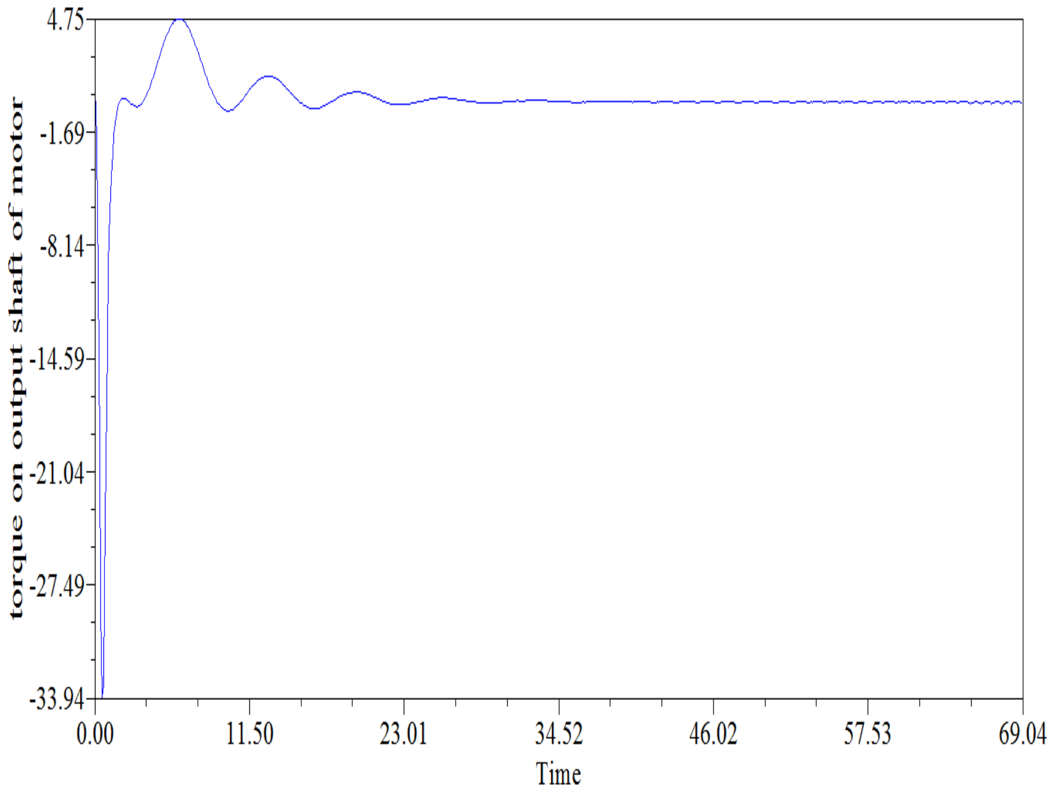

Fig 5.2: Motor output torque v/s time

The trend of variation of motor output torque is represented with respect to time in fig5.2. Figure 5.2 shows that initial high and negative torque can be thought as the starting torque of motor which under a constant power supply attains positive value which also tends to stabilize at 46.02s.

5.3 FORCE ON BOGIE:

In a single coach, there are two bogies and each bogie has 2 set of wheels. But here modeling is done while considering only a single set of wheel and thus load has been changed accordingly. It can be seen in fig 5.3 that bogie is relatively taking a longer time of 69.04s to stabilize which in a way seems to be justified as it is interacting with two types of force, one its self-load and second, the force transferred on it via wheels (which is taking a relatively longer time to achieve stability). So it takes a little bit longer to stabilize which can be changed by changing the stiffness of spring.

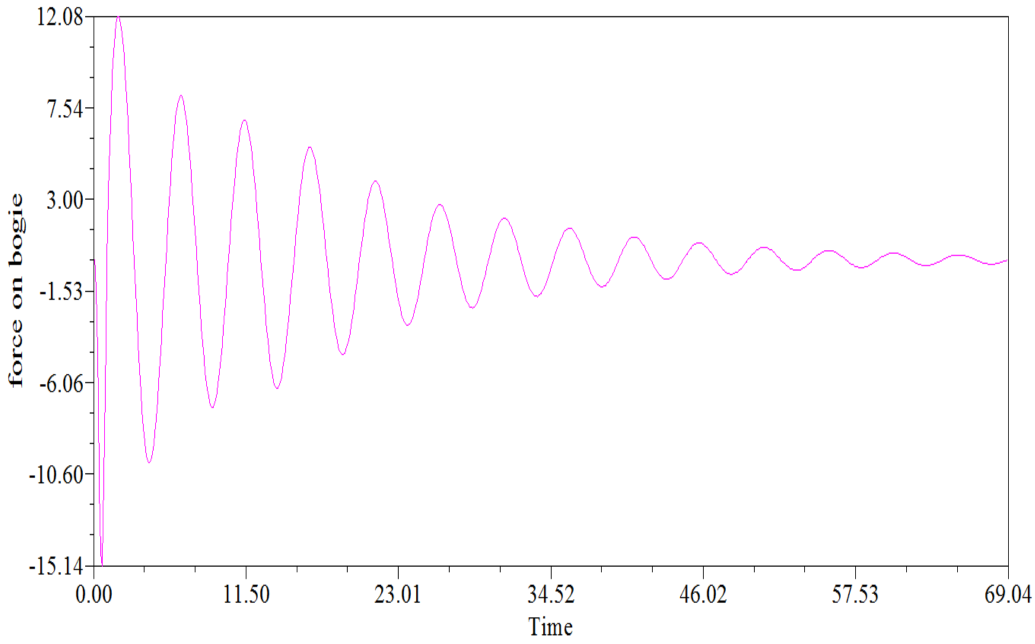

Fig

Fig. 5.3: Force on bogie v/s time.

5.4 MOMENTUM OF WHEEL:

It can be seen in fig 5.4, representing momentum of wheel with time, that wheel takes quite a longer time to stabilize, almost as 1.5 times that of motor. It takes 70.12s to achieve a stable momentum.

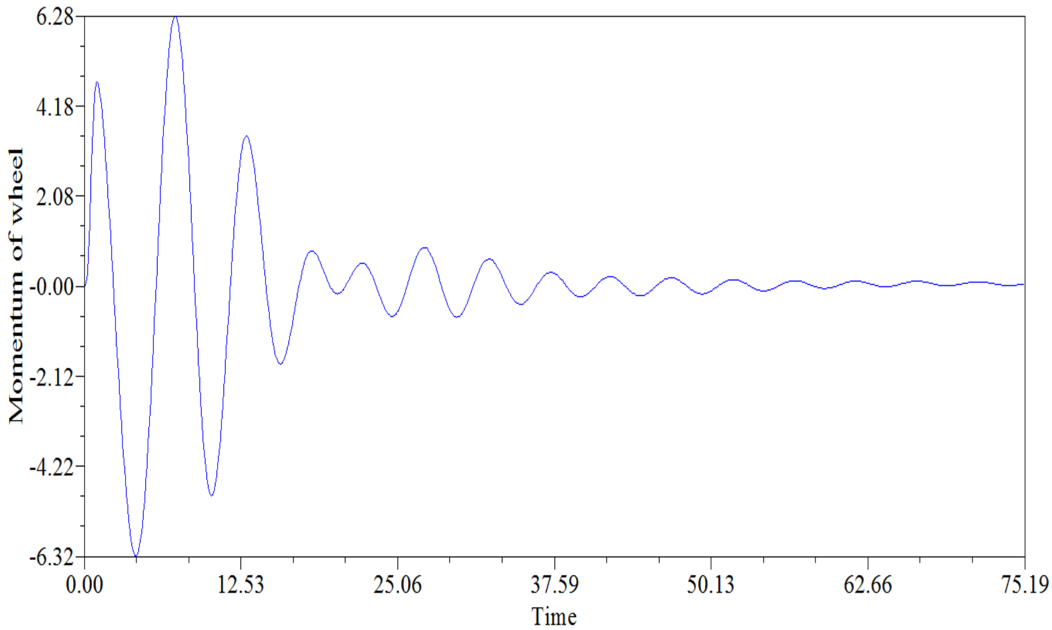

Fig 5.4: Momentum of wheel

5.5 TRACTION FORCE ON WHEELS:

A high traction force at start of time is observed in fig 5.5, because body is just step in motion. Generally, as the speed increases, traction forces tend to decrease. They both tend to stabilize within an interval of 1.5s of each other.

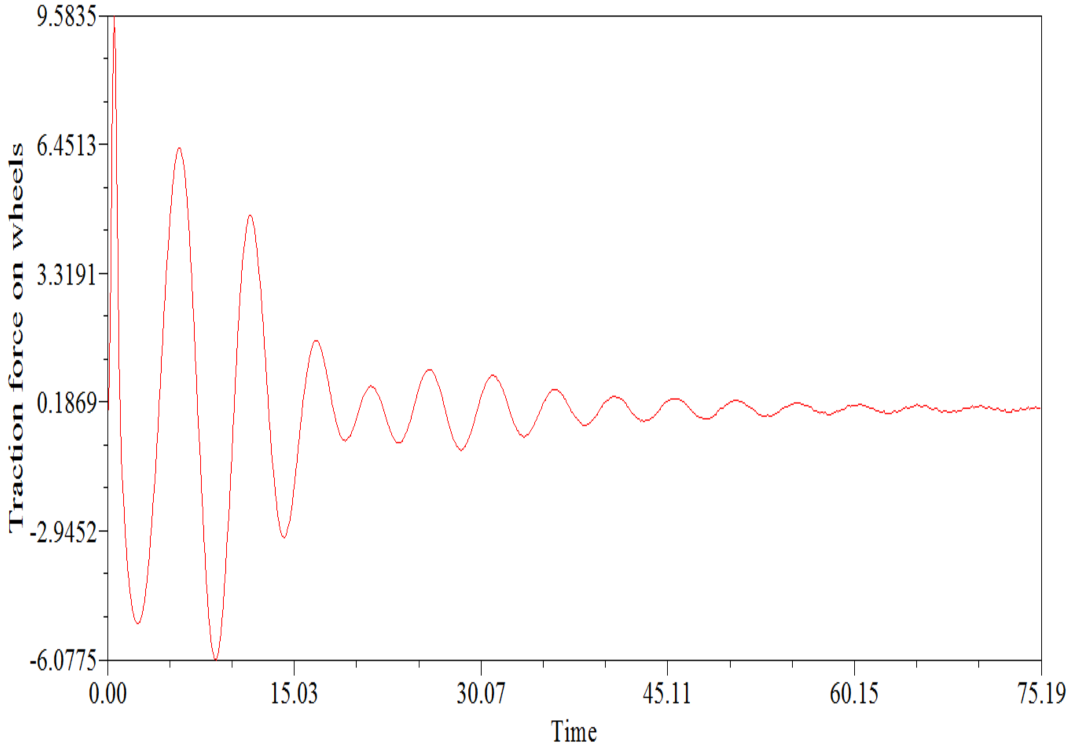

Fig 5.5: Traction force on wheel v/s time.

5.6 COMPARISON OF MOMENTUM AND TRACTION FORCE:

When fig 5.5 and 5.6 are plotted on a single graph in figure 5.7, it is observed that the system (wheels) momentum and traction are in synchronization, which shall be the case as well as per newton's second law i.e. rate of change of momentum is force. So there is just a phase difference.

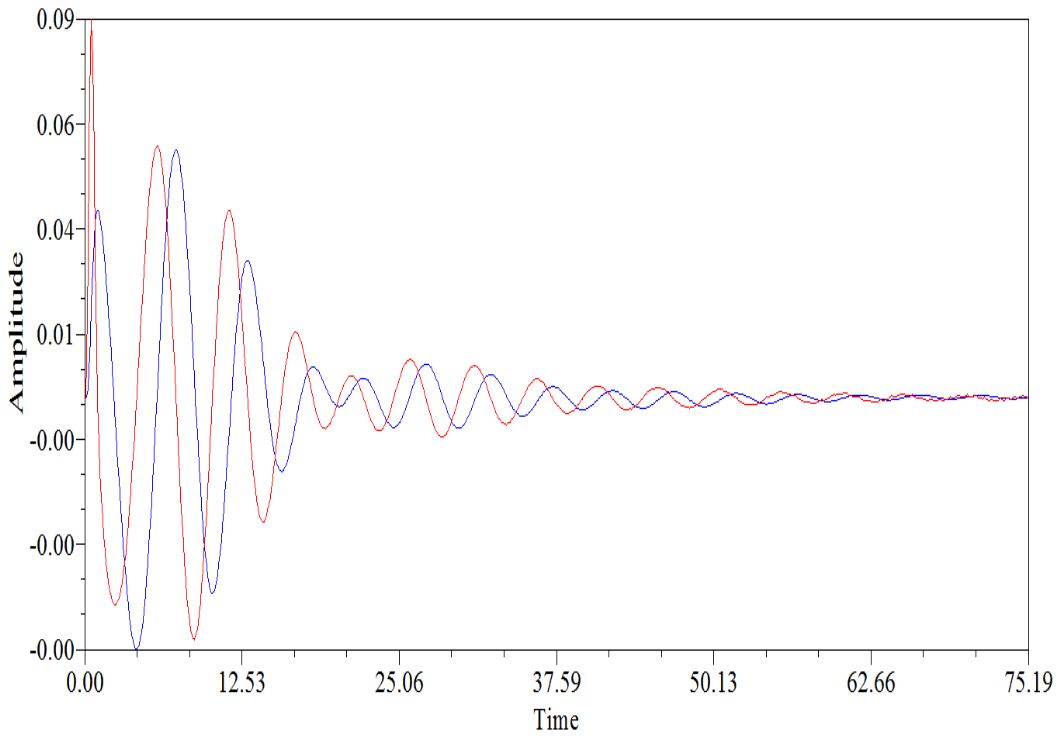

Fig 5.6: Traction force and momentum v/s time.

(Red plot: Traction force, Blue Plot: Momentum)

CHAPTER 6

CONCLUSION AND RESULTS

6.1 RESULTS:

Arr1=1/motorme1_NrQ1*(-motorme1_I18d/dt(1/motorme1_NrQ1*De6_Measurement)-1/ motorme _NrQ1*De6_Measurement*motorme1_rrotor+De4_Measurement)-1/motorme1_I68*intg(De6_measurement)-De6_Measurement/motorme1_Rload1

Arr2=1/motorel1_Nr*(-1/motorel1_/Nr*De5_Measurement*motorel1_Rcore-1/motorel1_C40*intg(1/motorel1_Nr*De5_Measurement))

Arr3=(1/motorel1_C5*intg(1/motorel_1Nr*De4_Measurement)+1/motorel1_Nr*De4_Measurement* motorel1_Rcore)/motorel1_Ns-(-motorel1_Ns/motorel_Nr*de4_Measurement-motorel1_I15*d/dt((1/motorel1_C5*intg(1/motorel1_Nr*De4_Measurement)+1/motorel1_Nr*De4_ Measurement*motorel1_Rcore)/motorel1_Ns)+voltage1_SE1)/motorel1_Rstator

Arr4=voltage1_SE1-De1_Measurement

Arr5=voltage3_SE1-De3_Measurement

Arr6=1/WHEEL1_TF*De6_Measurement-De7_Measurement

Arr7=voltage2_SE1-De2_Measurement

6.2 CONCLUSION:

- The model of a EMU traction system with load of a bogie shared by one set of wheel has been created and simulated on bondgraph.
- It was observed that the wheel attains a stable value of momentum as well as traction force in around 70.12s after the system has been turned on i.e. power has been supplied.
- For generation of ARR 7 sensors were placed at the chosen location (mainly at junctions) through which ARR has been generated which helps in detection of fault.
- These ARR so generated can be used to generate a Fault Signature Matrix (FSM) which may be further used to detect and isolate the fault.

6.3 FUTURE SCOPE

This technique is compatible with different formats of fault diagnosis methodologies. Therefore, it can be very helpful in developing a framework where analytical and experimental data can be collectively evaluated and observed. In context to that, the relative error can be manifested and may be linked to the control algorithms so that faults can be detected, isolated and controlled which will further reduce the possibility of catastrophic failure of a particular system. This technique can also be used for removing redundancy from the systems by analyzing least fault pattern.

Further faults can be obtained and compared with the help of ARR generated and an online control system can be developed which manifests itself with respect to the possibility propagation of fault and even fault can be isolated. More intense model can also be generated with more exact data.

REFERENCES

1. D. Cho, J. K. Hedrick, "Automotive Powertrain Modeling for Control", Journal of Dynamic Systems, Measurement, and Control, Vol. 111, no. 4, pp. 568-576, Dec 1989.

2. J. F. Broenink, “Introduction to Physical Systems Modelling with Bond Graphs”, Control Laboratory, University of Twente, Netherland, 1999, pp. 1-31.

3. M. Staroswiecki, "quantitative and qualitative models for fault detection and isolation", mechanical systems and signal processing, Vol. 14, no. 3,pp. 301-325,2000.

4. A. Mukherjee, A.K. Samantaray, " System Modeling through Bond graph Objects on SYMBOLS 2000", in Proc. International conference on bond graph modeling and simulation, vol. 33, pp. 164-170, 2001.

5. C. C. Chan, "The State of the Art of Electric and Hybrid Vehicles", In proc. of IEEE, vol 90,no.2,pp. 247-275,Feb. 2002.

6. A.K. Samantaray, B. OuldBuamama, , M. Staroswiecki, G. Dauphin-Tanguy, "Derivation of constraint relations from bond graph models for fault detection and isolation", SIMULATION SERIES, Vol. 33, no. 2, pp. 2-7, Jan 2003.

7. G Filippini , N. Nigro , and S. Junco, "Vehicular mediante bond graphs", Mecánica, Vol. 24, pp. 1559-1582, June 2004.

8. A. K. Samantaray, B. Ouldbouamama, K. Medjaher "component-based modelling of thermofluid systems for sensor placement and fault detection", Vol. 80 no. 7-8, page(s): 381-398, July 2004.

9. A.K. Samantaraya, B. Ould Bouamama, G.Tanguyc, K. Medjahera, M. Staroswieckib , " Model builder using functional and bond graphtools for FDI design", Control Engineering Practice, vol. 13, pp. 875-891, nov. 2004.

10. A.K. Samantaray, B. Conrard, B. Ould Bouamama*, K. Medjaher, M. Bayart, "Fault detection and isolation of smart actuators using bond graphs and external models", Control Engineering Practice, vol. 13, pp. 159-175, march 2004.

11. G. Filippini, N. Nigro and S. Junc, " Vehicle dynamics simulation using bond graphs", Facultad de Ciencias Exactas, vol. 1, pp. 2-12, January 2005.

12. A.K. Samantaraya, B. Ouldbouamamaa, G. Dauphin, K. Medjahera, M. Staroswieckib, "model builder using functional and bondgraph tools for fdi design",Vol. 13, pp. 875-891,2005.

13. A.K. Samantaray, B. Ould Bouamama, G.Tanguy K. Medjaher, M. Staroswiecki," Diagnostic bond graphs for online fault detection and isolation", Simulation Modelling Practice and Theory,vol. 14, pp. 237-262,July 2005.

14. B. Sareni, G. Gandanegara1, G. Tanguy, X. Roboam, "Bond-graph-based model simplification for system analysis: application to a railway traction device", Journal of Systems and Control engineering , Vol. 220, no. 7, pp. 553-571, Nov. 2006.

15. A. K. Samantaray, B. Ouldbouamama, G. Dauphin, K. Medjaher, M. Staroswiecki, "Diagnostic bond graphs for online fault detection and isolation", simulation modelling practice and theory, Vol. 14,pp. 237-262, 2006.

16. B. Ould-bouamama, K. Medjaher, M.A. Djeziri, R. Merzouki, "Backlash fault detection in mechatronic system", international journal of mechatronics, Vol. 17,No. 6, pp. 299-310, 2007.

17. A.K. Samantaray, S.K. Ghoshal, "Bicausal bond graphs for supervision: From fault detection and isolation to fault accommodation", Journal of the Franklin Institute, vol. 345, pp. 1–28, may 2007.

18. P. C. Breedveld," Modeling and Simulation of Dynamic Systems Using Bond Graphs", Control Systems Robotics and Automation, vol 4, pp. 1-37, Jan. 2008.

19. K. Samantaray, S.K. Ghoshal, "Bicausal bond graphs for supervision: from fault detection and isolation to fault accommodation, journal of the franklin institute, vol. 345, pp. 1-28, 2008.

20. V. Kumar,V. Rastogi , "Investigation of vertical dynamic behaviour and modelling of a typical Indian rail road vehicle through bond graph", World Journal of Modelling and Simulation, vol. 5,no. 2, pp. 130-138, 2009.

21. W. Borutzky, "Bond graph modelling and simulation of multidisciplinary systems ", An introduction Simulation Modelling Practice and Theory, vol. 17, pp. 3–21, 2009.

22. G. Romero, J. Felez, J. Maroto, J.M. Mera, "Efficient simulation of mechanism kinematics using bond graphs", Simulation Modelling Practice and Theory, vol. 17, pp.293–308, 2009.

23. H. K. Fathy, J. L. Stein, T. Ersal, "Structural simplification of modular bond-graph models based on junction inactivity", Simulation Modelling Practice and Theory, vol. 17, pp. 175–196, 2009.

24. A.K Samantaray, B. Ouldbouamama, K. Medjaher, M. Bayart, "Fault detection and isolation of smart actuators using bond graphs and external models", control engineering practice, vol. 13, pp. 159-175, 2009.

25. B. U. Rai, I. Umanand, "Bond graph toolbox for handling complex variable", IET control theory and applications, Vol 3, no. 5, pp. 551-560, April 2009.

26. B. Cai, B. Ning, H. Dong, Z.Hou, "Automatic Train Control System Development and Simulation for High-Speed Railways", IEEE Circuits And Systems Magazine, vol. 10, no. 2, pp. 6 - 18, 2010.

27. H. Peng, S. Wu, X. Huang, Z.Yang "Traction Technology for Chinese Railways", in Proc. International Power Electronics Conference, pp. 2842-2848, August 2010.

28. B. Jiang, H. Yang, V. Cocquempot, "Optimal Fault-Tolerant Path-Tracking Control for 4WS4WD Electric Vehicles", IEEE Transactions On Intelligent Transportation Systems, VOL. 11, NO. 1, pp. 237 - 243, March 2010.

29. J. Wang, R. Wang, "Fault-Tolerant Control With Active Fault Diagnosis for Four-Wheel Independently Driven Electric Ground Vehicles", IEEE Transactions on vehicular technology, vol. 60, no. 9, pp. 4276-4287, November 2011.

30. A. Namaane, K. Sia, N. K. M'sirdi "A New Structural Approach For Arrs Generation From Linear & Linearized Bond Graphs", In Proc. International Conference On Communications, Computing And Control Applications (Ccca), pp. 1-4, Sept 2011

31. P.M. Pathak, V. Kumar, V. Rastogi "Computational Analysis of Railway Vehicle on Irregular Tracks", International Conference on "Bond Graph Modeling and Simulation (ICBGM-14)", 6-10 July 2014.

32. B. M Ouldbouamama, R. Merzouki, "Extension of the bond graph causality inversion method for fault detection and isolation", Mechatronics, vol. 24, no. 8, pp. 1042-1049, Dec. 2014.

33. B. Jiang, Hindawi, N. Lu, Y. Wu, Y. Zhou, "Modeling of High-Speed Railway Traction Device", 18th International Conference on Intelligent Transportation Systems, pp. 1345-1350, 2015.

34. W. Cai, Y.D. Song, Y. Li, "Neuro-Adaptive Fault-Tolerant Approach for Active Suspension Control of High-Speed Trains", IEEE Transactions On Intelligent Transportation Systems, Vol. 16, NO. 5, pp. 2446 - 2456, Oct. 2015.

35. M. Naim, N. Harun, Yusran, "The Effect of Modifying Stator Winding in 1-Phase 4-Pole Starting Capacitor Induction Motor in Table Drill Machine on Current, Power

and Rotation of The Rotor", IOSR Journal of Electrical and Electronics Engineering, vol. 10, no. 4, pp. 91-97, Aug 2015.

36. G. Varga, M. Staroswiecki, “Analytical redundancy relations for fault detection and isolation", Automatica, vol. 31, no.5, pp. 687-699, May 2015.

37. Abdessalambadoud, M. Khemliche, S. Latrèche, “Bond graph modelling for fault detection and isolation of an ultrasonic linear motor", vol 1583-0233, no. 16, pp. 125-144, June 2016.

38. http://www.railway-technical.com/trains/rolling-stock-index-l/electric-locomotives.html

39. https://en.wikipedia.org/wiki/Electric_multiple_unit#Types

40. http://www.railway-technical.com/trains/rolling-stock-index-l/train-equipment/electric-traction-control-d.html

41. https://groups.csail.mit.edu/drl/journal_club/papers/Samantaray__2001__www.bondgraphs.com_about

42. https://www.eolss.net/Sample-Chapters/C18/E6-43-07-04.pdf

APPENDIX

Please note: 'd' represents the time derivative of the state variable within the first parenthesis.

ID1=
1/(1+1/WHEEL11_R14/WHEEL11_TF*gearbox1_R12/WHEEL11_TF+1/WHEEL11_R14/WHEEL11_TF /gearbox1_m*gearbox1_R3/gearbox1_m/WHEEL11_TF)

ID2=
1/(11/WHEEL12_R14/WHEEL12_TF*gearbox1_R12/WHEEL11_TF*ID1/WHEEL11_R14/WHEEL11_TF *gearbox1_R12/WHEEL12_TF-1/WHEEL12_R14/WHEEL12_TF*gearbox1_R12/WHEEL11_TF *ID1/WHEEL11_R14/WHEEL11_TF/gearbox1_m*gearbox1_R3/gearbox1_m/WHEEL12_TF +1/WHEEL12_R14/WHEEL12_TF*gearbox1_R12/WHEEL12_TF-1/WHEEL12_R14/WHEEL12_TF/gearbox1_m*gearbox1_R3/gearbox1_m/WHEEL11_TF*ID1/WHEEL11_R14/WHEEL11_TF *gearbox1_R12/WHEEL12_TF-1/WHEEL12_R14/WHEEL12_TF/gearbox1_m*gearbox1_R3 /gearbox1_m/WHEEL11_TF*ID1/WHEEL11_R14/WHEEL11_TF/gearbox1_m*gearbox1_R3 /gearbox1_m/WHEEL12_TF+1/WHEEL12_R14/WHEEL12_TF/gearbox1_m*gearbox1_R3/gearbox1_m /WHEEL12_TF)

ID3=
ID2/WHEEL12_R14/WHEEL12_TF*gearbox1_K11*gearbox1_Q11+ID2/WHEEL12_R14/WHEEL12_TF*gearbox1_R12/WHEEL11_TF*ID1/WHEEL11_R14/WHEEL11_TF*gearbox1_K11*gearbox1_Q11+ID2/WHEEL12_R14/WHEEL12_TF*gearbox1_R12/WHEEL11_TF*ID1/WHEEL11_R14/WHEEL11_TF*gearbox1_R12/WHEEL11_TF*WHEEL11_P16/WHEEL11_M16+ID2/WHEEL12_R14/WHEEL12_TF*gearbox1_R12/WHEEL11_TF*ID1/WHEEL11_R14/WHEEL11_TF*gearbox1_R12/WHEEL11_TF*P14/M14+ID2/WHEEL12_R14/WHEEL12_TF*gearbox1_R12/WHEEL11_TF*ID1/WHEEL11_R14/WHEEL11_TF*gearbox1_R12/WHEEL12_TF*WHEEL12_P16/WHEEL12_M16+ID2/WHEEL12_R14 /WHEEL12_TF*gearbox1_R12/WHEEL11_TF*ID1/WHEEL11_R14/WHEEL11_TF*gearbox1_R12 /WHEEL12_TF*P15/M15-ID2/WHEEL12_R14/WHEEL12_TF*gearbox1_R12/WHEEL11_TF*ID1/WHEEL11_R14/WHEEL11_TF/gearbox1_m*gearbox1_R3*gearbox1_P15/gearbox1_M15+ID2/WHEEL12_R14/WHEEL12_TF*gearbox1_R12/WHEEL11_TF*ID1/WHEEL11_R14/WHEEL11_TF/gearbox1_m*gearbox1_R3/

gearbox1_m/WHEEL11_TF*WHEEL11_P16/WHEEL11_M16+ID2/WHEEL12_R14/WHEEL12_TF*gearbox1_R12/WHEEL11_TF*ID1/WHEEL11_R14/WHEEL11_TF/gearbox1_m*gearbox1_R3/gearbox1_m/WHEEL11_TF*P14/M14+ID2/WHEEL12_R14/WHEEL12_TF*gearbox1_R12/WHEEL11_TF*ID1/WHEEL11_R14/WHEEL11_TF/gearbox1_m*gearbox1_R3/gearbox1_m/WHEEL12_TF*WHEEL12_P16/WHEEL12_M16+ID2/WHEEL12_R14/WHEEL12_TF*gearbox1_R12/WHEEL11_TF*ID1/WHEEL11_R14/WHEEL11_TF/gearbox1_m*gearbox1_R3/gearbox1_m/WHEEL12_TF*P15/M15ID2/WHEEL12_R14/WHEEL12_TF*gearbox1_R12/WHEEL11_TF*ID1/WHEEL11_R14/WHEEL11_TF/gearbox1_m*gearbox1_R3/gearbox1_m*gearbox1_P19/gearbox1_M19ID2/WHEEL12_R14/WHEEL12_TF*gearbox1_R12/WHEEL11_TF*ID1/WHEEL11_R14/WHEEL11_TF/gearbox1_m*gearbox1_K4*gearbox1_Q4+ID2/WHEEL12_R14/WHEEL12_TF*gearbox1_R12/WHEEL11_TF*ID1/WHEEL11_R14/WHEEL11_TF/gearbox1_m*motorme1_NrQ2*motorme1_P57/motorme1_M57+ID2/WHEEL12_R14/WHEEL12_TF*gearbox1_R12/WHEEL11_TF*ID1/WHEEL11_R14/WHEEL11_TF/gearbox1_m*motorme1_NrQ1*motorme1_P18/motorme1_M18+ID2/WHEEL12_R14/WHEEL12_TF*gearbox1_R12/WHEEL11_TF*ID1/WHEEL11_R14/WHEEL11_TF/BOGIE11_tf2*BOGIE11_K8*BOGIE11_Q8+ID2/WHEEL12_R14/WHEEL12_TF*gearbox1_R12/WHEEL11_TF*ID1/WHEEL11_R14/WHEEL11_TF*BOGIE11_tf3*BOGIE11_K11*BOGIE11_Q11+ID2/WHEEL12_R14/WHEEL12_TF*gearbox1_R12/WHEEL11_TF*ID1/WHEEL11_R14*WHEEL11_K15*WHEEL11_Q15ID2/WHEEL12_R14/WHEEL12_TF*gearbox1_R12/WHEEL11_TF*WHEEL11_P16/WHEEL11_M16ID2/WHEEL12_R14/WHEEL12_TF*gearbox1_R12/WHEEL11_TF*P14/M14-ID2/WHEEL12_R14/WHEEL12_TF*gearbox1_R12/WHEEL12_TF*WHEEL12_P16/WHEEL12_M16-ID2/WHEEL12_R14/WHEEL12_TF*gearbox1_R12/WHEEL12_TF*P15/M15+ID2/WHEEL12_R14/WHEEL12_TF/gearbox1_m*gearbox1_R3*gearbox1_P15/gearbox1_M15+ID2/WHEEL12_R14/WHEEL12_TF/gearbox1_m*gearbox1_R3/gearbox1_m/WHEEL11_TF*ID1/WHEEL11_R14/WHEEL11_TF*gearbox1_K11*gearbox1_Q11+ID2/WHEEL12_R14/WHEEL12_TF/gearbox1_m*gearbox1_R3/gearbox1_m/WHEEL11_TF*ID1/WHEEL11_R14/WHEEL11_TF*gearbox1_R12/WHEEL11_TF*WHEEL11_P16/WHEEL11_M16+ID2/WHEEL12_R14/WHEEL12_TF/gearbox1_m*gearbox1_R3/gearbox1_m/WHEEL11_TF*ID1/WHEEL11_R14/WHEEL11_TF*gearbox1_R12/WHEEL11_TF*P14/M14+ID2/WHEEL12_R14/WHEEL12_TF/gearbox1_m*gearbox1_R3/gearbox1_m/WHEEL11_TF*ID1/WHEEL11_R14/WHEEL11_TF*gearbox1_R12/WHEEL12_TF*WHEEL12_P16/WHEEL12_M16+ID2/WHEEL12_R14/WHEEL12_TF/gearbox1_m*gearbox1_R3/gearbox1_m/WHEEL11_TF*ID1/WHEEL11_R14/WHEEL11_TF*gearbox1_R12/WHEEL12_TF*P15/M15-ID2/WHEEL12_R14/WHEEL12_TF/gearbox1_m*gearbox1_R3/gearbox1_m/WHEEL11_TF*ID1/WHEEL11_R14/WHEEL11_TF/gearbox1_m*gearbox1_R3*gearbox1_P15/gearbox1_M15+ID2/WHEEL12_R14/WHEEL12_TF/gearbox1_m*gearbox1_R3/gearbox1_m/WHEEL11_TF*ID1/WHEEL11_R14/WHEEL11_TF/gearbox1_m*gearbox1_R3/gearbox1_m/WHEEL11_TF*WHEEL11_P16/WHEEL11_M16+ID2/WHEEL12_R14/WHEEL12_TF/gearbox1_m*gearbox1_R3/gearbox1_m/WHE

EL11_TF*ID1/WHEEL11_R14/WHEEL11_TF/gearbox1_m*gearbox1_R3/gearbox1_m/WHEEL11_TF*P14/M14+ID2/WHEEL12_R14/WHEEL12_TF/gearbox1_m*gearbox1_R3/gearbox1_m/WHEEL11_TF*ID1/WHEEL11_R14/WHEEL11_TF/gearbox1_m*gearbox1_R3/gearbox1_m/WHEEL12_TF*WHEEL12_P16/WHEEL12_M16+ID2/WHEEL12_R14/WHEEL12_TF/gearbox1_m*gearbox1_R3/gearbox1_m/WHEEL11_TF*ID1/WHEEL11_R14/WHEEL11_TF/gearbox1_m*gearbox1_R3/gearbox1_m/WHEEL12_TF*P15/M15ID2/WHEEL12_R14/WHEEL12_TF/gearbox1_m*gearbox1_R3/gearbox1_m/WHEEL11_TF*ID1/WHEEL11_R14/WHEEL11_TF/gearbox1_m*gearbox1_R3/gearbox1_m*gearbox1_P19/gearbox1_M19-
ID2/WHEEL12_R14/WHEEL12_TF/gearbox1_m*gearbox1_R3/gearbox1_m/WHEEL11_TF*ID1/WHEEL11_R14/WHEEL11_TF/gearbox1_m*gearbox1_K4*gearbox1_Q4+ID2/WHEEL12_R14/WHEEL12_TF/gearbox1_m*gearbox1_R3/gearbox1_m/WHEEL11_TF*ID1/WHEEL11_R14/WHEEL11_TF/gearbox1_m*motorme1_NrQ2*motorme1_P57/motorme1_M57+ID2/WHEEL12_R14/WHEEL12_TF/gearbox1_m*gearbox1_R3/gearbox1_m/WHEEL11_TF*ID1/WHEEL11_R14/WHEEL11_TF/gearbox1_m*motorme1_NrQ1*motorme1_P18/motorme1_M18+ID2/WHEEL12_R14/WHEEL12_TF/gearbox1_m*gearbox1_R3/gearbox1_m/WHEEL11_TF*ID1/WHEEL11_R14/WHEEL11_TF/BOGIE11_tf2*BOGIE11_K8*BOGIE11_Q8+ID2/WHEEL12_R14/WHEEL12_TF/gearbox1_m*gearbox1_R3/gearbox1_m/WHEEL11_TF*ID1/WHEEL11_R14/WHEEL11_TF*BOGIE11_tf3*BOGIE11_K11*BOGIE11_Q11+ID2/WHEEL12_R14/WHEEL12_TF/gearbox1_m*gearbox1_R3/gearbox1_m/WHEEL11_TF*ID1/WHEEL11_R14*WHEEL11_K15*WHEEL11_Q15-
ID2/WHEEL12_R14/WHEEL12_TF/gearbox1_m*gearbox1_R3/gearbox1_m/WHEEL11_TF*WHEEL11_P16/WHEEL11_M16 -
ID2/WHEEL12_R14/WHEEL12_TF/gearbox1_m*gearbox1_R3/gearbox1_m/WHEEL11_TF*P14/M14-ID2/WHEEL12_R14/WHEEL12_TF/gearbox1_m*gearbox1_R3/gearbox1_m/WHEEL12_TF*WHEEL12_P16/WHEEL12_M16-
ID2/WHEEL12_R14/WHEEL12_TF/gearbox1_m*gearbox1_R3/gearbox1_m/WHEEL12_TF*P15/M15+ID2/WHEEL12_R14/WHEEL12_TF/gearbox1_m*gearbox1_R3/gearbox1_m*gearbox1_P19/gearbox1_M19+ID2/WHEEL12_R14/WHEEL12_TF/gearbox1_m*gearbox1_K4*gearbox1_Q4-
ID2/WHEEL12_R14/WHEEL12_TF/gearbox1_m*motorme1_NrQ2*motorme1_P57/motorme1_M57-
ID2/WHEEL12_R14/WHEEL12_TF/gearbox1_m*motorme1_NrQ1*motorme1_P18/motorme1_M18-ID2/WHEEL12_R14/WHEEL12_TF/BOGIE11_tf2*BOGIE11_K8 *BOGIE11_Q8-
ID2/WHEEL12_R14/WHEEL12_TF*BOGIE11_tf3*BOGIE11_K11*BOGIE11_Q11 -
ID2/WHEEL12_R14*WHEEL12_K15*WHEEL12_Q15

ID4=ID1/WHEEL11_R14/WHEEL11_TF*gearbox1_K11*gearbox1_Q11ID1/WHEEL11_R14/WHEEL11_TF*gearbox1_R12/WHEEL11_TF*WHEEL11_P16/WHEEL11_M16ID1/WHEEL11_R14/WHEEL11_TF *gearbox1_R12/WHEEL11_TF*P14/M14-

ID1/WHEEL11_R14/WHEEL11_TF*gearbox1_R12/WHEEL12_TF*ID3ID1/WHEEL11_R14/WHEEL11_TF*gearbox1_R12/WHEEL12_TF*WHEEL12_P16 /WHEEL12_M16-ID1/WHEEL11_R14/WHEEL11_TF*gearbox1_R12/WHEEL12_TF*P15/M15+ID1/WHEEL11_R14/WHEEL11_TF/gearbox1_m*gearbox1_R3*gearbox1_P15/gearbox1_M15 -ID1/WHEEL11_R14/WHEEL11_TF/gearbox1_m*gearbox1_R3/gearbox1_m/WHEEL11_TF *WHEEL11_P16/WHEEL11_M16-ID1/WHEEL11_R14/WHEEL11_TF/gearbox1_m*gearbox1_R3/gearbox1_m/WHEEL11_TF*P14/M14ID1/WHEEL11_R14/WHEEL11_TF/gearbox1_m*gearbox1_R3/gearbox1_m/WHEEL12_TF*ID3-ID1/WHEEL11_R14/WHEEL11_TF/gearbox1_m*gearbox1_R3/gearbox1_m/WHEEL12_TF*WHEEL12_P16/WHEEL12_M16-ID1/WHEEL11_R14/WHEEL11_TF/gearbox1_m*gearbox1_R3/gearbox1_m/WHEEL12_TF*P15/M15+ID1/WHEEL11_R14/WHEEL11_TF/gearbox1_m*gearbox1_R3/gearbox1_m*gearbox1_P19/gearbox1_M19+ID1/WHEEL11_R14/WHEEL11_TF/gearbox1_m*gearbox1_K4*gearbox1_Q4-ID1/WHEEL11_R14/WHEEL11_TF/gearbox1_m*motorme1_NrQ2*motorme1_P57/motorme1_M57-ID1/WHEEL11_R14/WHEEL11_TF/gearbox1_m*motorme1_NrQ1*motorme1_P18/motorme1_M18-ID1/WHEEL11_R14/WHEEL11_TF /BOGIE11_tf2*BOGIE11_K8*BOGIE11_Q8-ID1/WHEEL11_R14/WHEEL11_TF*BOGIE11_tf3 *BOGIE11_K11*BOGIE11_Q11-ID1/WHEEL11_R14*WHEEL11_K15*WHEEL11_Q15

ID5=gearbox1_R12/WHEEL11_TF*ID4+gearbox1_R12/WHEEL11_TF*WHEEL11_P16/WHEEL11_M16+gearbox1_R12/WHEEL11_TF*P14/M14+gearbox1_R12/WHEEL12_TF*ID3+gearbox1_R12/WHEEL12_TF*WHEEL12_P16/WHEEL12_M16+gearbox1_R12/WHEEL12_TF*P15/M15

ID6= gearbox1_R3*gearbox1_P15/gearbox1_M15-gearbox1_R3/gearbox1_m/WHEEL11_TF *ID4-gearbox1_R3/gearbox1_m/WHEEL11_TF*WHEEL11_P16/WHEEL11_M16-gearbox1_R3/gearbox1_m/WHEEL11_TF*P14/M14-gearbox1_R3/gearbox1_m/WHEEL12_TF*ID3-gearbox1_R3/gearbox1_m/WHEEL12_TF*WHEEL12_P16/WHEEL12_M16gearbox1_R3/gearbox1_m/WHEEL12_TF *P15/M15+gearbox1_R3/gearbox1_m*gearbox1_P19/gearbox1_M19

d(P15)= 1/WHEEL12_TF*(-gearbox1_K11*gearbox1_Q11-ID5-1/gearbox1_m*(-ID6-gearbox1_K4*gearbox1_Q4+motorme1_NrQ2*motorme1_P57/motorme1_M57+motorme1_NrQ1*motorme1_P18 /motorme1_M18)-1/BOGIE11_tf2*BOGIE11_K8*BOGIE11_Q8-BOGIE11_tf3*BOGIE11_K11 *BOGIE11_Q11) d(P14) =1/WHEEL11_TF*(-gearbox1_K11*gearbox1_Q11-ID5-1/gearbox1_m*(-ID6gearbox1_K4*gearbox1_Q4+motorme1_NrQ2*motorme1_P57/motorme1_M57+motorme1_NrQ1*motorme1_P18 /motorme1_M18)-1/BOGIE11_tf2*BOGIE11_K8*BOGIE11_Q8-BOGIE11_tf3*BOGIE11_K11 *BOGIE11_Q11)

d(WHEEL12_P16)=
1/WHEEL12_TF*(-gearbox1_K11*gearbox1_Q11-ID5-1/gearbox1_m*(-ID6-gearbox1_K4 *gearbox1_Q4+motorme1_NrQ2*motorme1_P57/motorme1_M57+motorme1_NrQ1*motorme1_P18 /motorme1_M18)-1/BOGIE11_tf2*BOGIE11_K8*BOGIE11_Q8-BOGIE11_tf3*BOGIE11_K11 *BOGIE11_Q11)

d(WHEEL12_Q15)= ID3

d(WHEEL11_P16)=
1/WHEEL11_TF*(-gearbox1_K11*gearbox1_Q11-ID5-1/gearbox1_m*(-ID6-gearbox1_K4 *gearbox1_Q4+motorme1_NrQ2*motorme1_P57/motorme1_M57+motorme1_NrQ1*motorme1_P18 /motorme1_M18)-1/BOGIE11_tf2*BOGIE11_K8*BOGIE11_Q8-BOGIE11_tf3*BOGIE11_K11 *BOGIE11_Q11)

d(WHEEL11_Q15)= ID4

d(BOGIE11_P25)=
-1/BOGIE11_tf2*BOGIE11_K8*BOGIE11_Q8-BOGIE11_tf3*BOGIE11_K11*BOGIE11_Q11

d(BOGIE11_P17)=
1/BOGIE11_tf4*BOGIE11_K11*BOGIE11_Q11-BOGIE11_R20*BOGIE11_P17/BOGIE11_M17 -BOGIE11_K21*BOGIE11_Q21

d(BOGIE11_P5) =
-BOGIE11_K3*BOGIE11_Q3-BOGIE11_R4*BOGIE11_P5/BOGIE11_M5+BOGIE11_tf1*BOGIE11_K8 *BOGIE11_Q8

d(BOGIE11_Q21)= BOGIE11_P17/BOGIE11_M17

d(BOGIE11_Q11) =
BOGIE11_tf3*(1/WHEEL11_TF*(ID4+WHEEL11_P16/WHEEL11_M16+P14/M14)+1/WHEEL12

_TF*(ID3+WHEEL12_P16/WHEEL12_M16+P15/M15)+BOGIE11_P25/BOGIE11_M25)-1/BOGIE11_tf4 *BOGIE11_P17/BOGIE11_M17

d(BOGIE11_Q8) = -BOGIE11_tf1*BOGIE11_P5/BOGIE11_M5+1/BOGIE11_tf2*(1/WHEEL11_TF*(ID4+WHEEL11_P16/WHEEL11_M16+P14/M14)+1/WHEEL12_TF*(ID3+WHEEL12_P16/WHEEL12_M16+P15/M15) +BOGIE11_P25/BOGIE11_M25)

d(BOGIE11_Q3) =BOGIE11_P5/BOGIE11_M5

d(gearbox1_P19) =
1/gearbox1_m*(-ID6-gearbox1_K4*gearbox1_Q4+motorme1_NrQ2*motorme1_P57/motorme1_M57+motorme1_NrQ1*motorme1_P18/motorme1_M18)

d(gearbox1_P15)=-ID6-gearbox1_K4*gearbox1_Q4+motorme1_NrQ2*motorme1_P57/motorme1_M57+motorme1_NrQ1*motorme1_P18/motorme1_M18

d(gearbox1_Q11)=
1/WHEEL11_TF*(ID4+WHEEL11_P16/WHEEL11_M16+P14/M14)+1/WHEEL12_TF*(ID3+WHEEL12_P16 /WHEEL12_M16+P15/M15)

d(gearbox1_Q4)= gearbox1_P15/gearbox1_M15+1/gearbox1_m*(-1/WHEEL11_TF*(ID4+WHEEL11_P16/WHEEL11_M16 +P14/M14)-1/WHEEL12_TF*(ID3+WHEEL12_P16/WHEEL12_M16+P15/M15)+gearbox1_P19 /gearbox1_M19)

d(motorme1_P68)=
motorme1_NrQ2*motorme1_P57/motorme1_M57+motorme1_NrQ1*motorme1_P18/motorme1_M18

d(motorme1_P57)=
-motorme1_R58*motorme1_P57/motorme1_M57+motorel1_Nr/motorel1_R6*(-motorel1_cos120 *motorel1_Ns*motorel1_P27/motorel1_M27-motorel1_cos240*motorel1_Ns*motorel1_P23/motorel1_M23+motorel1_Ns*motorel1_P15/motorel1_M15-motorel1_Nr*motorme1_P57 /motorme1_M57-motorel1_K5*motorel1_Q5)-

motorme1_NrQ2*(motorme1_P68/motorme1_M68+gearbox1_P15/gearbox1_M15+1/gearbox1_m*(-1/WHEEL11_TF*(ID4+WHEEL11_P16 /WHEEL11_M16+P14/M14)-1/WHEEL12_TF*(ID3+WHEEL12_P16/WHEEL12_M16+P15/M15) +gearbox1_P19/gearbox1_M19)+1/motorme1_R70*(motorme1_NrQ2*motorme1_P57/motorme1_M57 +motorme1_NrQ1*motorme1_P18/motorme1_M18))

d(motorme1_P18)=
-motorme1_R19*motorme1_P18/motorme1_M18+motorel1_Nr/motorel1_R11*(-motorel1_sin120*motorel1_Ns*motorel1_P27/motorel1_M27+motorel1_sin240*motorel1_Ns*motorel1_P23/motorel1_M23-motorel1_K40*motorel1_Q40-motorel1_Nr*motorme1_P18/motorme1_M18)-motorme1_NrQ1*(motorme1_P68/motorme1_M68+gearbox1_P15/gearbox1_M15+1/gearbox1_m*(-1/WHEEL11_TF*(ID4+WHEEL11_P16/WHEEL11_M16+P14/M14)-1/WHEEL12_TF*(ID3+WHEEL12_P16/WHEEL12_M16+P15/M15)+gearbox1_P19/gearbox1_M19)+1/motorme1_R70*(motorme1_NrQ2*motorme1_P57/motorme1_M57+motorme1_NrQ1*motorme1_P18/motorme1_M18))

d(motorme1_Q66)= 0

d(motorme1_Q65)= 0

d(motorel1_P57)= 0

d(motorel1_P56)= 0

d(motorel1_P15)=
-motorel1_Ns/motorel1_R6*(-motorel1_cos120*motorel1_Ns*motorel1_P27/motorel1_M27 -motorel1_cos240*motorel1_Ns*motorel1_P23/motorel1_M23+motorel1_Ns*motorel1_P15 /motorel1_M15-motorel1_Nr*motorme1_P57/motorme1_M57-motorel1_K5*motorel1_Q5) -motorel1_R13*motorel1_P15/motorel1_M15+voltage1_SE1

d(motorel1_P27)= -motorel1_Ns*(-motorel1_cos120/motorel1_R6*(-motorel1_cos120*motorel1_Ns*motorel1_P27/motorel1_M27-motorel1_cos240*motorel1_Ns*motorel1_P23/motorel1_M23+motorel1_Ns*motorel1_P15/motorel1_M15-motorel1_Nr*motorme1_P57/motorme1_M57 -motorel1_K5*motorel1_Q5)-motorel1_sin120/motorel1_R11*(-motorel1_sin120 *motorel1_Ns*motorel1_P27/motorel1_M27+motorel1_sin240*motorel1_Ns*motorel1_P23

/motorel1_M23-motorel1_K40*motorel1_Q40-motorel1_Nr*motorme1_P18/motorme1_M18))
-motorel1_R25*motorel1_P27/motorel1_M27+voltage2_SE1

d(motorel1_P23)= -motorel1_Ns*(motorel1_sin240/motorel1_R11*(-motorel1_sin120*motorel1_Ns
*motorel1_P27/motorel1_M27+motorel1_sin240*motorel1_Ns*motorel1_P23/motorel1_M23
-motorel1_K40*motorel1_Q40-motorel1_Nr*motorme1_P18/motorme1_M18) motorel1_cos240
/motorel1_R6*(-motorel1_cos120*motorel1_Ns*motorel1_P27/motorel1_M27-motorel1_cos240
*motorel1_Ns*motorel1_P23/motorel1_M23+motorel1_Ns*motorel1_P15/motorel1_M15
-motorel1_Nr*motorme1_P57/motorme1_M57-motorel1_K5*motorel1_Q5))-motorel1_R22
*motorel1_P23/motorel1_M23+voltage3_SE1

d(motorel1_Q40)=
1/motorel1_R11*(-motorel1_sin120*motorel1_Ns*motorel1_P27/motorel1_M27+motorel1_sin240
*motorel1_Ns*motorel1_P23/motorel1_M23-motorel1_K40*motorel1_Q40-motorel1_Nr
*motorme1_P18/motorme1_M18)